ASTIA AVAILABILITY NOTICE

Qualified requestors may obtain copies of this report from ASTIA. ASTIA release to OTS not authorized.

THIRD QUARTERLY REPORT

STUDY OF PULSED RADIATION EFFECTS ON MICROWAVE FERRITE DUPLEXERS

1 November 1962 to 31 January 1963

Report No. 3

Contract No. DA 36-039-SC-89113

Department of the Army Task Number OST 740000528

February 1963

Study effects of pulsed nuclear radiation on the operating characteristics of C-Band microwave coaxial ferrite Y-junction circulators and gyromagnetic coupling limiters

Prepared by:

J. P. Scheiwe
G. R. Harrison

Approved by:

Dr. E. W. Matthews

Protective marking to be removed 31 January 1966

SPERRY MICROWAVE ELECTRONICS COMPANY
DIVISION OF SPERRY RAND CORPORATION
CLEARWATER, FLORIDA

SJ-222-0041-3 Copy No. 19

FOR OFFICIAL USE ONLY

TABLE OF CONTENTS

LIST OF ILLUSTRATIONS

LIST OF ILLUSTRATIONS (Cont'd)

LIST OF ILLUSTRATIONS (Cont'd)

LIST OF TABLES

FOR OFFICIAL USE ONLY

LIST OF TABLES (Cont'd)

1. PURPOSE

The general purpose of this study is to determine the effects of pulsed nuclear radiation on the operating characteristics of C-band beacon ferrite duplexers wherein the components used to make up the duplexer are two C-band microwave coaxial ferrite Y-junction circulators and one gyromagnetic coupling limiter. The ferrite duplexer to be investigated was developed by Sperry Microwave Electronics Company under Contract No. DA36-039-SC-85330. Experimental radiation effects data are to be acquired for the duplexer and/or its components operating in a frequency range of 5.4 to 5.9 Gc and, initially, for an operating power level (at the klystron) of approximately 1 watt (considered low power operation).

Specifically, the aims of the third quarter of the study were the following:

- The planning and performance of a second series of experiments at the Sandia Pulsed Reactor Facility (SPRF) (during the week of January 14, 1963) involving: (1) primarily, an extensive irradiation of the individual duplexer components with particular attention focused on the three port, Y-junction circulator and (2) secondarily, preliminary studies of possible radiation effects in coaxial and rectangular waveguides necessary for high power microwave tests and (3) high voltage dc experiments (which from the standpoint of electric field intensity were meant to simulate high microwave power experiments).

- The reduction and analysis of the data recorded during the aforementioned experiments.

2. ABSTRACT

This report presents the results from the second series of radiation environment experiments conducted during the third quarter of the program. These experiments were performed to substantiate and extend the data on the duplexer components' behavior obtained during the first series of experiments. Data are also presented from preliminary investigations of the radiation effects in waveguide elements (which might be required for future high power tests) and static dc voltage experiments which were conducted to simulate possible high microwave power electric field intensities.

Briefly described and reviewed are procedures for testing the coaxial ferrite Y-junction circulator, the gyromagnetic coupling limiter, the internal magnet coaxial isolator and C-band waveguide elements at a microwave power of 100 milliwatts in the frequency range of 5.4 to 5.9 Gc. Also reviewed is the method used to perform the static dc voltage experiments involving tests of the microwave components mentioned above, various open ended connectors (potted and unpotted) and short pieces of open ended cable.

Photographs of oscilloscope traces showing radiation effects on the operating characteristics of the microwave components and leakage characteristics of the components

used in the dc experiments are presented. Quantitative interpretations of the data obtained by circuit calibration procedures are also presented.

Results of dosimetry provided by the SPRF are tabulated along with the radiation effects noted in the components investigated in each experiment.

3. PUBLICATIONS, LECTURES, REPORTS AND CONFERENCES

3.1 PUBLICATIONS

A letter presenting a summary of the results from the initial series of experiments conducted at the SPRF (during the week of September 10, 1962) has been prepared and is now in the process of being checked and cleared for publication.

3.2 LECTURES

None in this reporting period.

3.3 REPORTS

None in this reporting period.

3.4 CONFERENCES

A conference was held on November 5, 1962 at Sperry Microwave Electronics Company, Clearwater, Florida. In attendance were G. R. Barton and A. Hinchee of the Systems Test Equipment Section of Sperry and G. R. Harrison, J. C. Hoover and J. P. Scheiwe of the Advanced Microwave Techniques Section of Sperry.

The purpose of this meeting was to discuss and ascertain the possible availability of a high power C-band RF source. Such a source would be required for high power pulsed microwave experiments. Although no such unit is presently available to the program it was decided that a unit satisfactory for use in radiation experiments could be constructed.[1]

4. FACTUAL DATA

4.1 EXPERIMENTAL PROCEDURES AND DATA

4.1.1 Introduction

Descriptions of the circuits and methods used to monitor the microwave characteristics of the various components under test have been presented in detail in previous quarterly reports[2,3] issued for this study. Only a brief discussion of the circuits will be presented herein for the sake of definition and clarity as to where and how the various signals were detected. The majority of the measurements were made using circuits similar to the one illustrated in Figure 1. The signal detected at the secondary port of the 20db coupler (1), Figure 1, was used to monitor the behavior of the input cw signal and as such is hereafter referred to as the monitor signal. With the klystron producing greater than 2 watts at cw operation the unperturbed monitor signal level, as measured at the crystal detector output, was 0.25 milliwatts. The signal detected at the receiver port of the three-port circulator (2) was used to monitor any changes that might occur in the reflected power and as such is hereafter referred to as the VSWR signal. With the klystron producing greater than 2 watts at cw operation the unperturbed VSWR signal level, as measured at the crystal detector output, was 1.75 milliwatts. The return or output

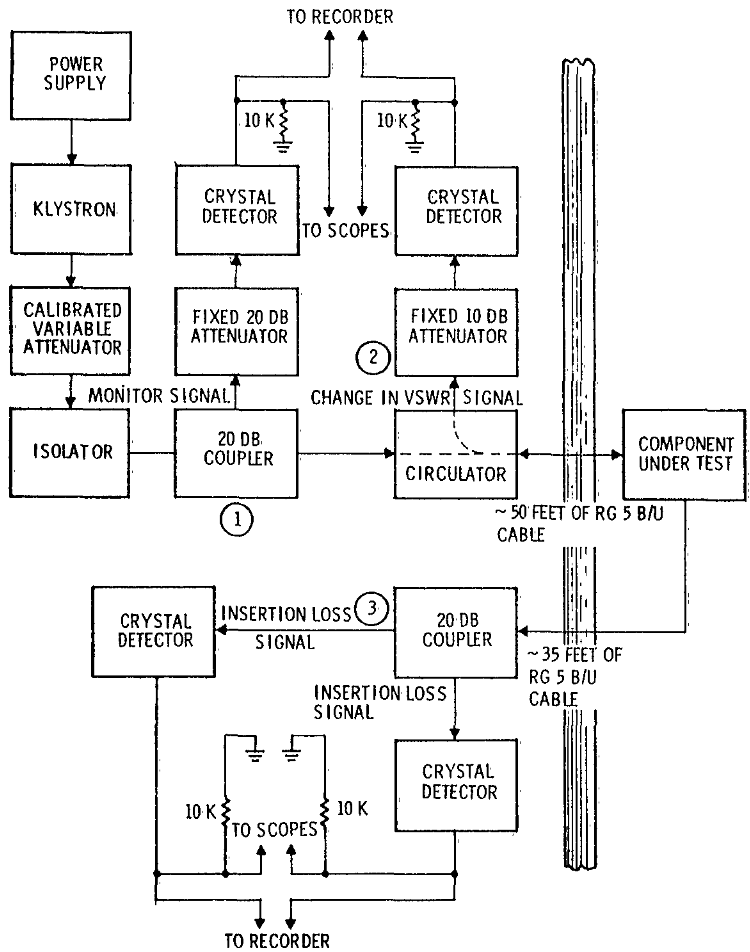

Figure 1. Typical Measurement Scheme for One Component in Low Power Tests

signal (labeled (3)) was monitored by feeding the signal directly into a crystal detector or by observing the signal 20 db down by use of a coupler as shown in Figure 1. In some cases both detectors were used. The signal level at the crystals was dependent on the component under test. During the course of the experimental program there were various planned changes made in the typical test circuit as shown in Figure 1. When waveguide sections were exposed, two waveguide-to-coax adapters were used inside the KIVA, one on each end of the waveguide element. This type of configuration is illustrated in Figures 2 and 3 which provide a close-up and broad view, respectively, of the aluminum and brass waveguide elements, one three-port circulator and the Sandia Pulsed Reactor in their respective test positions. Later changes in circuitry involved putting the entire front end of one circuit, less the klystron power supply, inside the KIVA adjacent to the device under test. This was done in order to deliver more power (approximately 1.75 watts) to certain selected devices. A circulator-limiter duplexer and a limiter, which begins its power limiting function at levels of 200 milliwatts and above, were tested at these higher powers. This particular test configuration is illustrated in Figures 4 and 5 which provide a close-up and broad "test position"

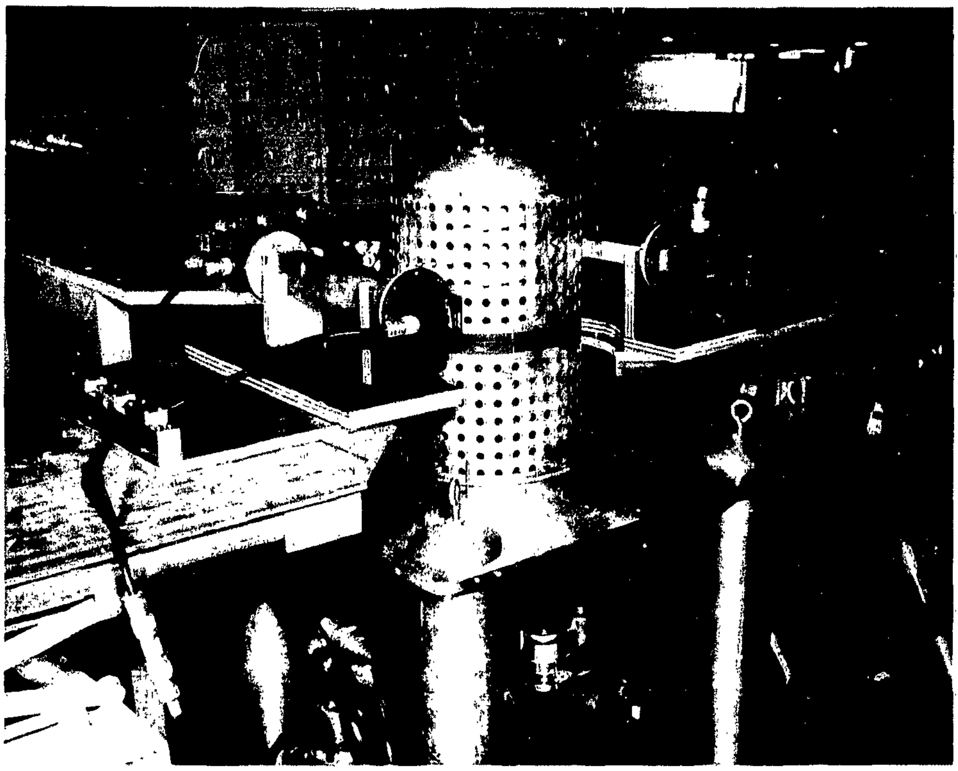

Figure 2. Close-Up View of Aluminum and Brass Waveguide Elements, One Test Three-Port Circulator and the Sandia Pulsed Reactor in Test Position

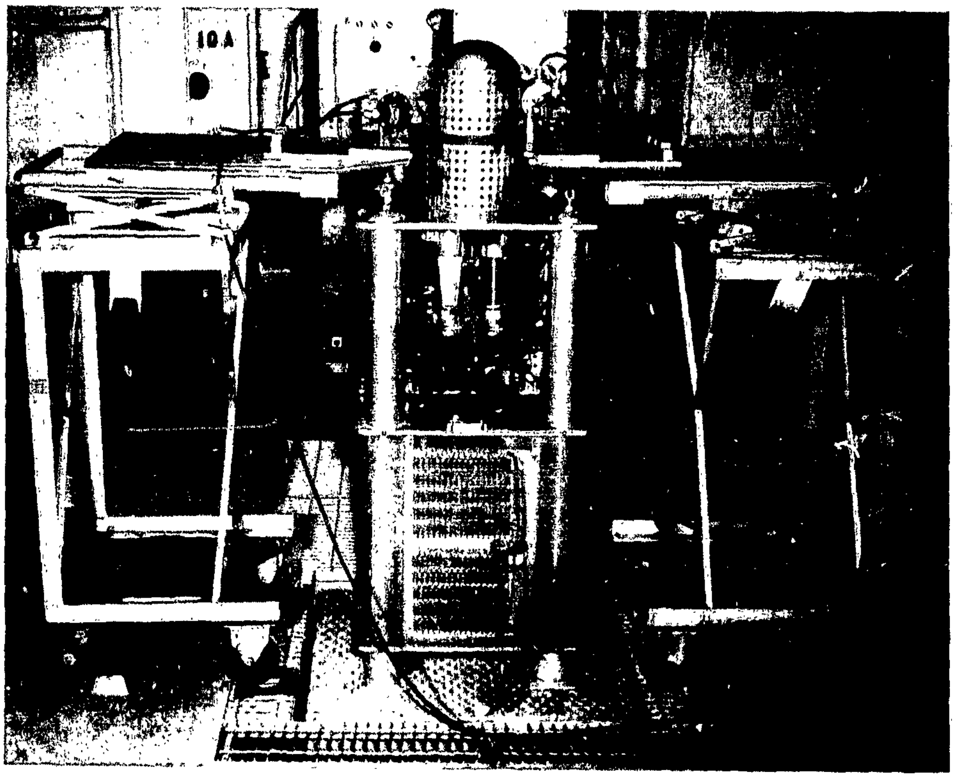

Figure 3. Broad View of Waveguide Elements and Circulator in Test Position With Conventional Cable Configurations of Figure 1

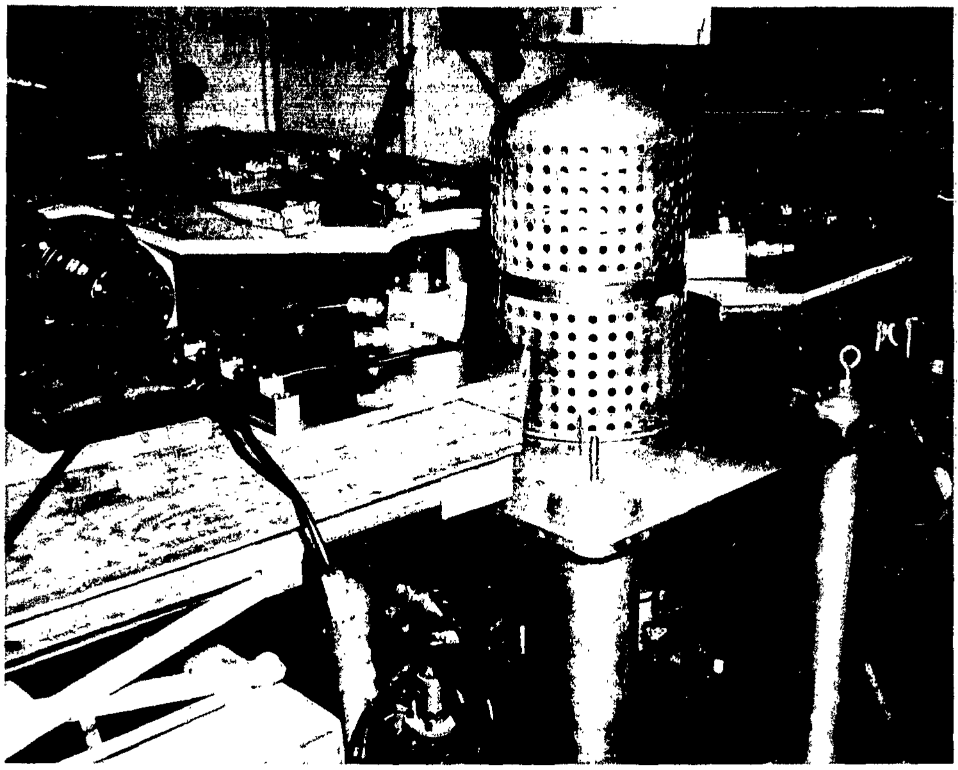

Figure 4. Close-Up View of Circulator-Limiter Duplexer Supplied by Circuit Front End in KIVA, Limiter, Three-Port Circulator and Sandia Pulsed Reactor in Test Position

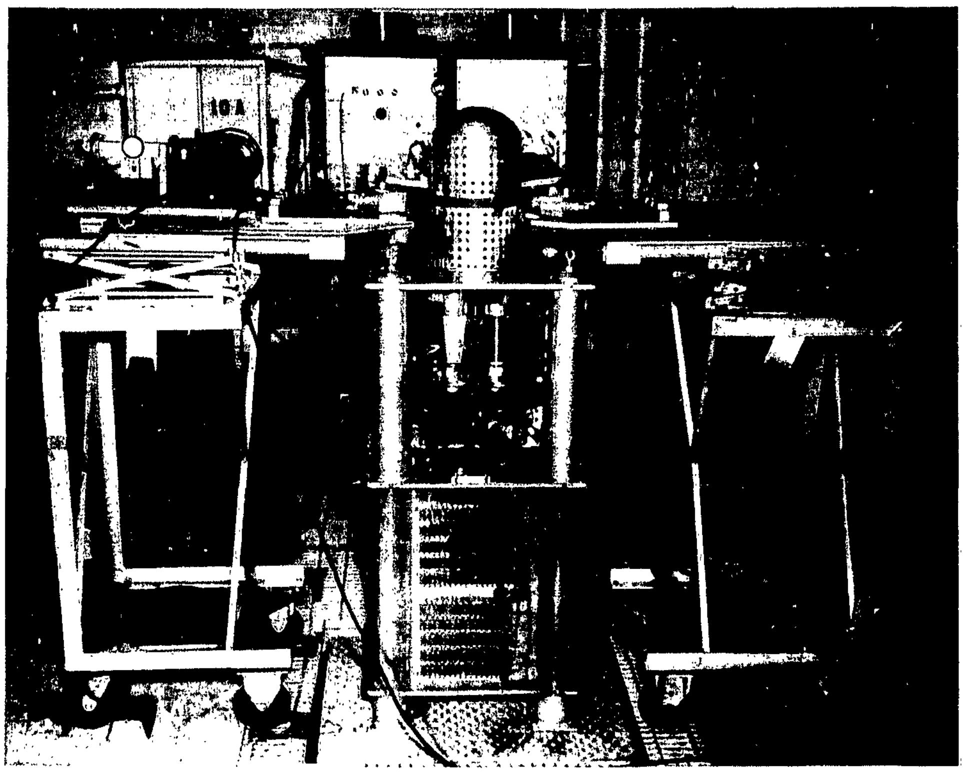

Figure 5. Broad View of Limiter, Circulator-Limiter Duplexer and Three-Port Circulator in Test Position With Front End in KIVA and Conventional Cable Configurations

view, respectively, of the circulator-limiter duplexer supplied by the circuit front end in the KIVA, a limiter tested in the conventional manner diagramed in Figure 1, a three-port circulator also tested in the conventional manner and the Sandia Pulsed Reactor.

Some experiments were performed with the crystal detectors placed directly on the output ports of the test components. This procedure was used only in cases where the components inherently provided a sufficient amount of power attenuation (namely, measurements of the isolation of a circulator or duplexer) between the input port and the port at which the measurement was made to guarantee that the crystal detector would not be saturated, i.e., power inputs to the detectors of less than 250 microwatts. Since it is quite possible that the radiation environment also affected the normal operation of the crystal detector, back up measurements of the appropriate microwave characteristics were performed whenever crystal detectors were placed inside the KIVA.

4.1.2 <u>High Voltage DC Experiments</u>

It was decided to perform high voltage dc experiments using microwave components, various connectors, and open ended cables in order to obtain quantitative data concerning possible leakage and/or voltage breakdown characteristics.

Particular attention was paid to devices and connectors where the ground plane is separated from the conductor by an air dielectric.

These dc voltage tests were meant to simulate the electric field that would be imposed on devices during high power microwave tests. To a reasonable approximation the power supplied to a microwave component may be expressed as

$$P = \frac{E^2}{Z}$$

where

P = power in watts

E = voltage (rms) in volts

Z = characteristic device impedence in ohms.

Since the voltage term is squared and a characteristic impedence of 50 ohms is common to microwave devices, relatively low (hundreds of volts) dc voltages may be used to simulate the electrical field produced by microwave powers up to ten killowatts.

A dc voltage supply was built and tested prior to the January test series. This supply used two 500 volt batteries in series as a voltage source. It was so constructed that two dc experiments with voltages variable in steps between 125 volts and 460 volts could be conducted

at the same time. The optional use of blocking diodes was available in the circuit to block out any undesirable transient oscillations that might ring in the transmission line if a complete short due to breakdown should occur at the reactor. Fifty-five feet of RG 58 C/U cable was used between the voltage supply and the component. In order to be able to display a complete 500 volt breakdown on the oscilloscopes which have a minimum vertical sensitivity of 50 volts/cm or less, a 100:1 voltage division between the voltage applied to the component and that displayed on the oscilloscopes (with 1 meg ohm input resistance in oscilloscopes and 10^5 ohm input resistance in Ampex recorders) was built into the supply unit. Further, since it was felt that the available surface area would affect the electron leakage characteristics of the test devices and cables, a negative or positive polarity option was built into the supply. Thus, in the case of cable tests the normal outside ground sheath could be made positive or negative with respect to the inside center conductor.

A circuit diagram of the dc voltage supply is presented in Figure 6. A photograph of the dc supply and two RG 58 C/U coaxial cables, one of which is connected to a half-potted type N double female connector and the other of which is connected to a half-potted BNC double female

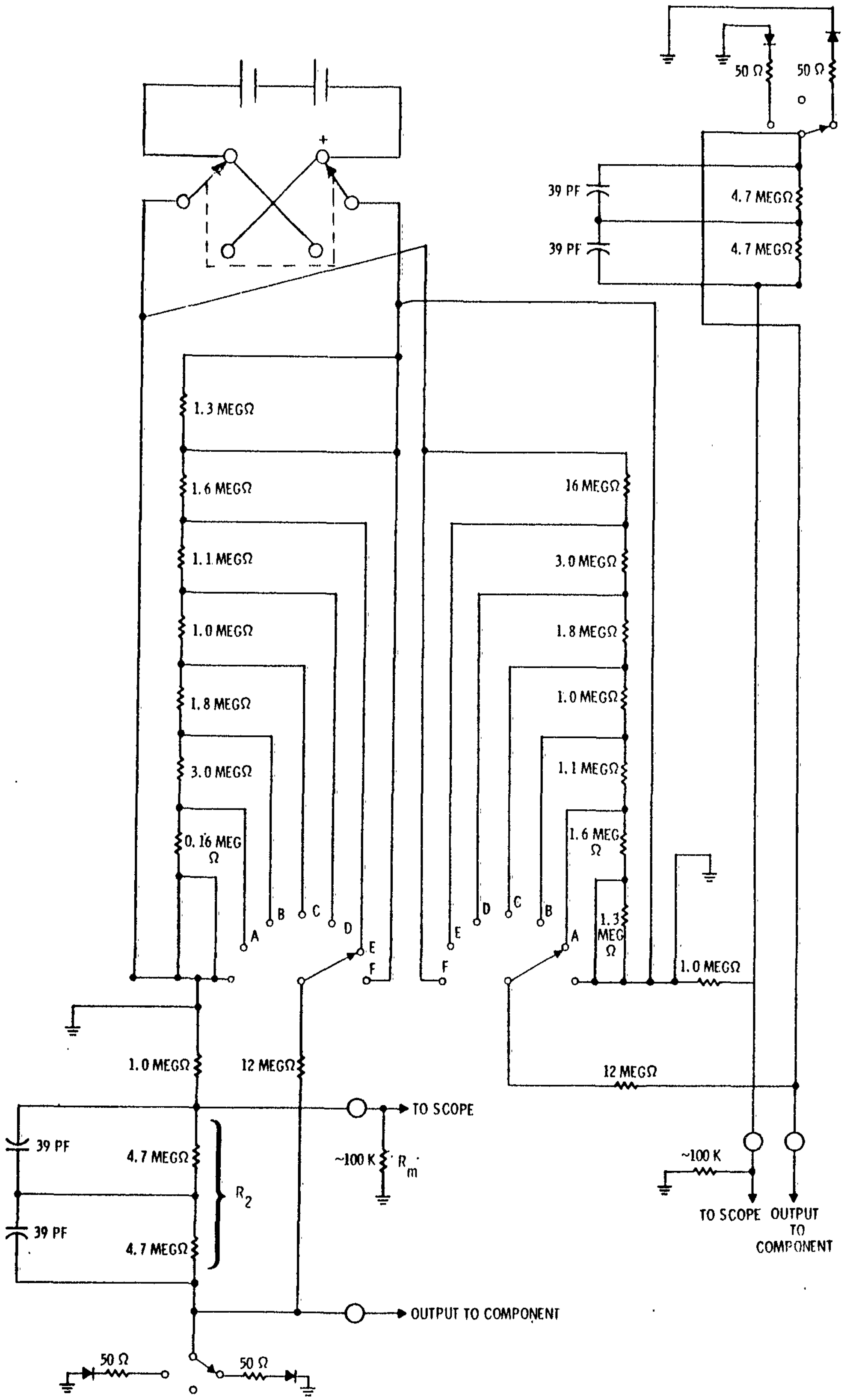

Figure 6. Circuit Diagram of dc High Voltage Supply

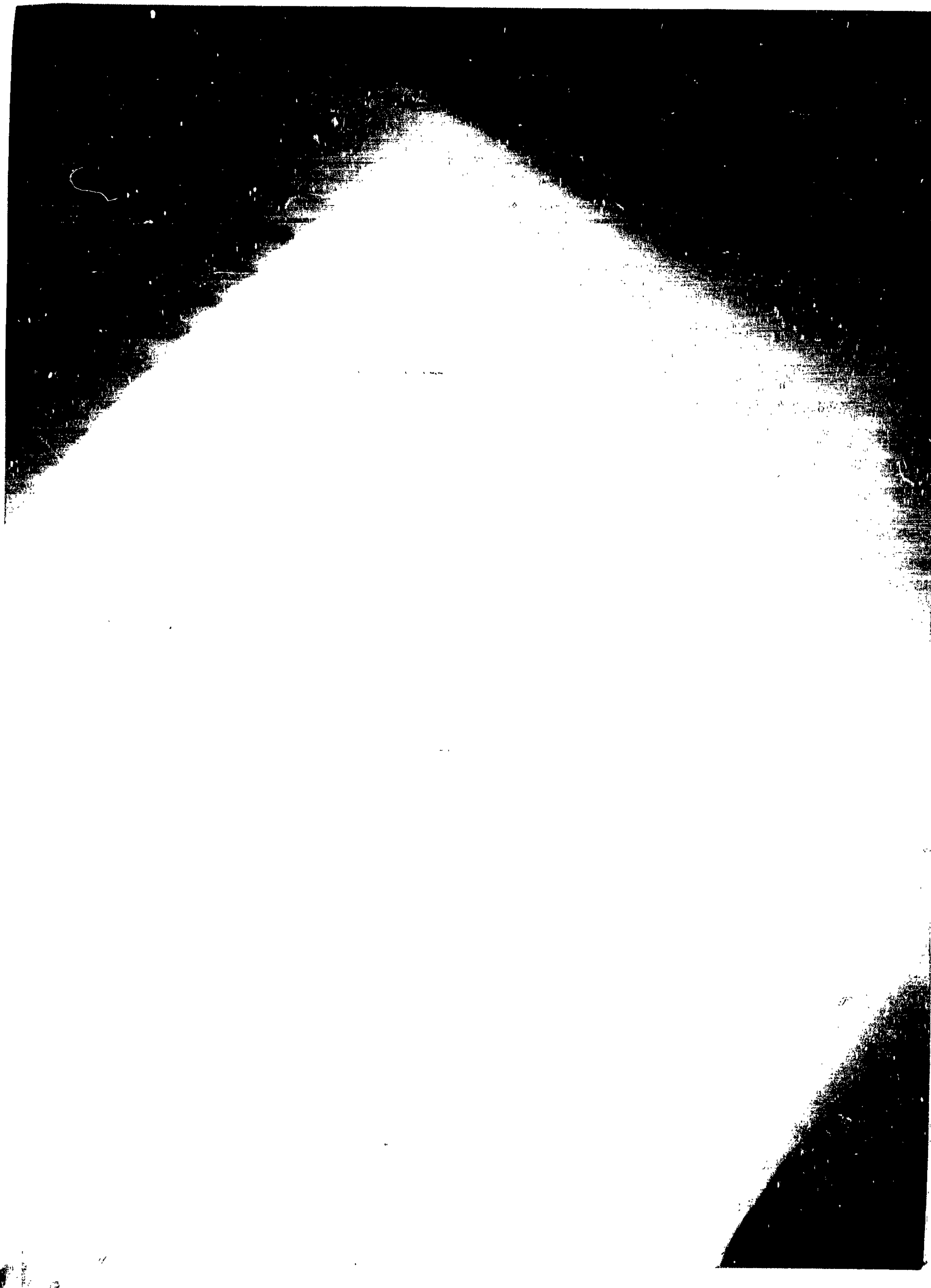

connector, is presented in Figure 7. Table 1 gives the voltage outputs for each graded step of the two channels to the components under test and to the oscilloscopes where the traces were displayed.

TABLE 1. GRADED VOLTAGE OUTPUT STEPS TO COMPONENTS AND OSCILLOSCOPES FROM THE DC VOLTAGE SUPPLY*

Steps	Output to Component #1, Volts (± 10 volts)	Output to Oscilloscope #1, Volts (± 0.1 volts)	Output to Component #2, Volts (± 10 volts)	Output to Oscilloscope #2, Volts (± 0.1 volts)
A	125	1.15	122	1.1
B	192	1.8	185	1.7
C	235	2.2	225	2.1
D	282	2.6	270	2.5
E	380	3.5	355	3.3
F	460	4.4	430	4.0

* Values shown are those used after the third burst.

Since the burst time of the Sandia Pulsed Reactor is of the order of 100 microseconds, it was felt that in order to guarantee resolution of events that might occur during the early part of the burst, the dc experimental circuit had to provide a resolution time of 10 microseconds or less. This feature was checked prior to the trip to Sandia by noting the response of the dc circuit to a superimposed 10 kc square wave. The results of this test are presented in Figure 8 wherein there is no apparent lag in the rise of the square wave pulse. It was concluded that the dc circuit had a sufficiently fast time response.

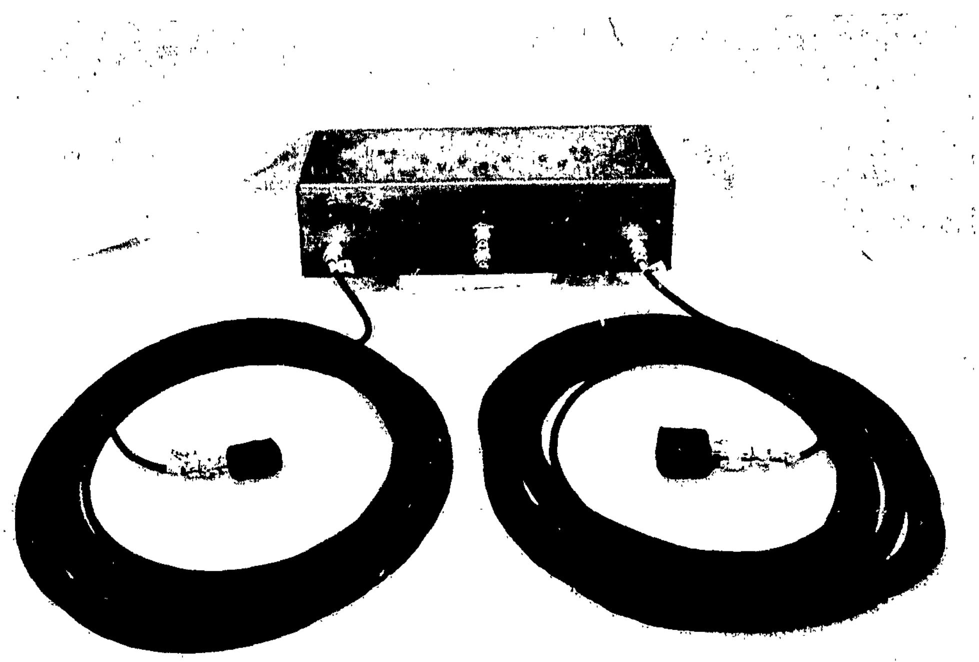

Figure 7. Photograph of High Voltage Supply and Half-Potted Type N and BNC Double Females in Test Configurations

4.1.3 Waveguide Tests

Two C-band waveguide elements, one made of brass and the other of aluminum, were tested (at 5.6 Gc) during this series of experiments so that a decision, based on experimental data, could be made regarding what type of transmission line to use in future high power tests. The waveguide elements were one foot in length and had a waveguide-to-coax adapter connected to each end. Tests were performed for each element using three different dielectrics; air, low density polystyrene shaped so as to fill all of the waveguide and adapter cavity, and high density polystyrene shaped in the same fashion as the low density polystyrene (See Figure 9). The properties of the polystyrenes (Styrofoam*) are listed in Table 2.

TABLE 2. PROPERTIES OF HIGH AND LOW DENSITY STYROFOAM DIELECTRICS USED IN WAVEGUIDE EXPERIMENTS

	High Density Styrofoam, HD-2	Low Density Styrofoam, Styrofoam-22
Density, lbs/ft^3	4.0 - 4.7	1.6 - 2.0
Dielectric Constant	1.07	<1.05
Disipation Factor	$<0.304 \times 10^{-3}$	$<0.302 \times 10^{-3}$
Contained Gas	Methyl Chloride, CH_3CL	Methyl Chloride CH_3CL

* Trade name, Dow Chemical Company

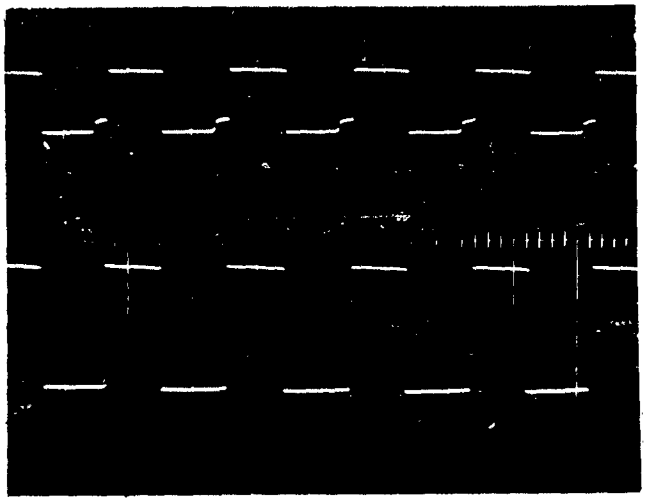

Upper Trace: Response With No Termination At Scope

Lower Trace: Response With 10 K Termination At Scope

Horizontal Sweep Time: 50 μsec/cm

Figure 8. Response of DC Experimental Circuit to Superimposed 10 KC Squarewave

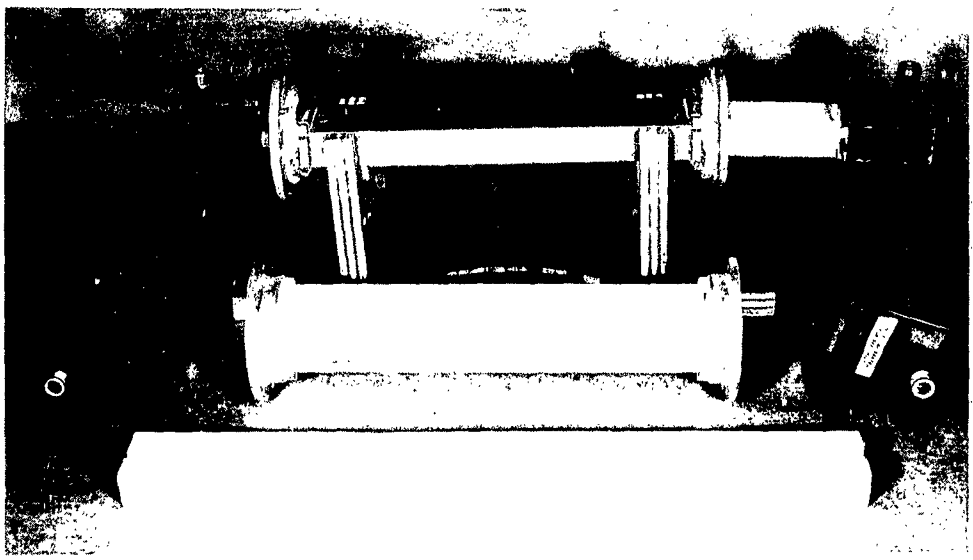

Figure 9. Photograph of Waveguide Elements Showing Styrofoam Inserts

Figures 10 through 15 are photographs representative of the data gathered for the radiation effects on waveguide elements from bursts 1 through 5. The lower trace on the first photograph (Figure 10) is the return signal from the brass waveguide with an air dielectric. The lower trace of the second photograph (Figure 11) is the return signal from the aluminum waveguide with an air dielectric. The single trace of the third photograph (Figure 12) is the return signal from the brass waveguide with a low density Styrofoam dielectric. This trace was obtained from a playback of the magnetic tape used to record the effects. The playback was necessary in this instance because the trace obtained on the oscilloscope at Sandia went off scale due to the unexpectedly large magnitude of the effect. The lower trace of the fourth photograph (Figure 13) is the return signal from the aluminum waveguide with a low density Styrofoam dielectric. The lower trace of the fifth photograph (Figure 14) is the return signal from the brass waveguide with a high density Styrofoam dielectric. The lower trace of the sixth photograph (Figure 15) is the return signal from the aluminum waveguide with a high density Styrofoam dielectric.

Tests were performed on two waveguide-to-coax adapters "butted together" in order to provide data with which to discriminate between the effects in the waveguide and the

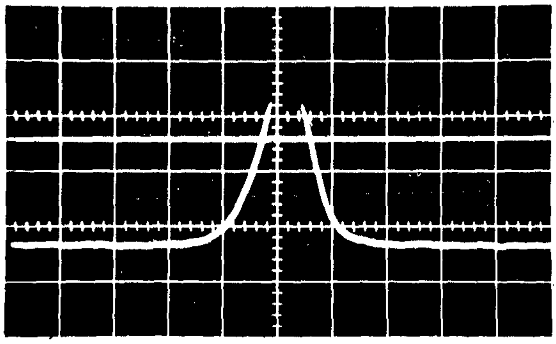

Upper Trace: Input Signal
Vertical Gain 0.05 volts/cm
Horizontal Sweep Speed 50 μsec/cm

Lower Trace: Return Signal
Vertical Gain 0.01 volts/cm
Horizontal Sweep Speed 50 μsec/cm

Figure 10. Burst No. 2, Waveforms of Input and Output Signals in Air Dielectric Filled Brass Waveguide Element

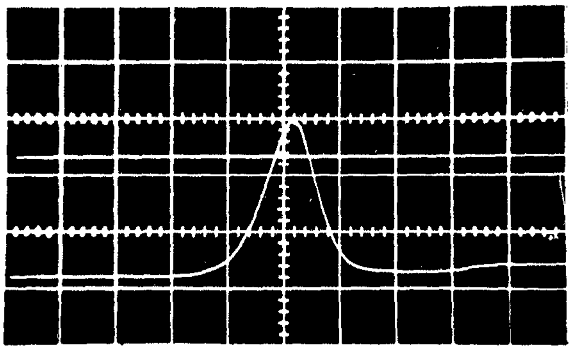

Upper Trace: Input Signal
Vertical Gain 0.05 volts/cm
Horizontal Sweep Speed 50 μsec/cm

Lower Trace: Return Signal
Vertical Gain 0.01 volts/cm
Horizontal Sweep Speed 50 μsec/cm

Figure 11. Burst No. 2, Waveforms of Input and Output Signals in Air Dielectric Filled Aluminum Waveguide Element

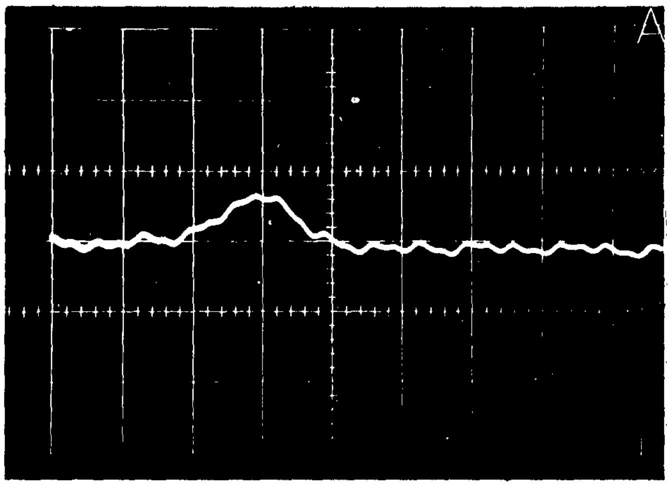

Return Signal
Vertical Gain 0.10 volts/cm
Horizontal Sweep Speed 50 μsec/cm

Figure 12. Burst No. 4, Waveform of Output Signal in Low Density Styrofoam Dielectric Filled Brass Waveguide Element

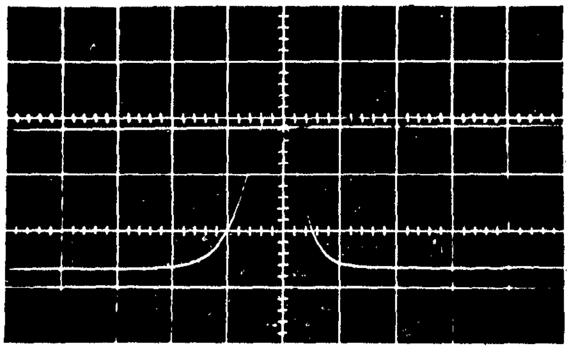

Upper Trace: Input Signal
Vertical Gain 0.05 volts/cm
Horizontal Sweep Speed 50 μsec/cm

Lower Trace: Return Signal
Vertical Gain 0.02 volts/cm
Horizontal Sweep Speed 50 μsec/cm

Figure 13. Burst No. 5, Waveforms of Input and Output Signals in Low Density Styrofoam Dielectric Filled Aluminum Waveguide Element

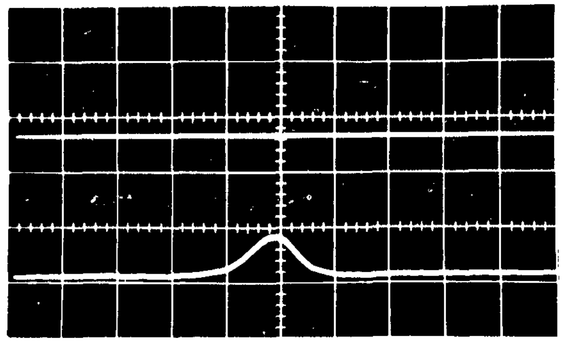

Upper Trace: Input Signal
Vertical Gain 0.05 volts/cm
Horizontal Sweep Speed 50 μsec/cm

Lower Trace: Return Signal
Vertical Gain 0.01 volts/cm
Horizontal Sweep Speed 50 μsec/cm

Figure 14. Burst No. 5, Waveforms of Input and Output Signal in High Density Styrofoam Dielectric Filled Brass Waveguide Element

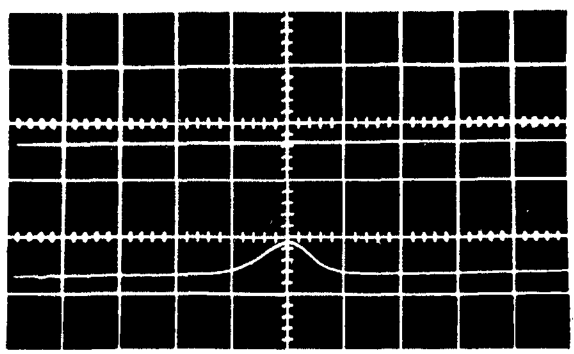

Upper Trace: Input Signal
Vertical Gain 0.05 volts/cm
Horizontal Sweep Speed 50 μsec/cm

Lower Trace: Return Signal
Vertical Gain 0.01 volts/cm
Horizontal Sweep Speed 50 μsec/cm

Figure 15. Burst No. 4, Waveforms of Input and Output Signal in High Density Styrofoam Dielectric Filled Aluminum Waveguide Element

effects in the waveguide-to-coax adapters. No photographs of this data are presented at this time, but the analysis of these and all other data from the waveguide tests will be discussed and tabulated in a later section of this report.

4.1.4 Component Tests

The C-band coaxial ferrite Y-junction circulator tests were performed using a single circulator and two circulators in tandem (the latter tests will be discussed in the section dealing with configurations involving more than one component) operating at frequencies of 5.4, 5.6 and 5.9 Gc and at power levels of 125 milliwatts and above.

Figures 16 and 17 are representative photographs of the circulator data obtained during the first through the sixteenth burst. Figure 16 (lower trace) is a photograph of the change in signal level detected during the tenth burst from the antenna port of a circulator operating at 5.6 Gc. The ripple appearing at the beginning and tail of the trace was caused by noise. A possible origin of this noise was found to be a difference in potential that existed between the metal conduit running under the KIVA wall and the ground sheath of some of the connectors joining RG 5 B/U cable sections. This condition will be rectified in future tests through the use of a large insulating rubber sleeve in which all cables going through the conduit

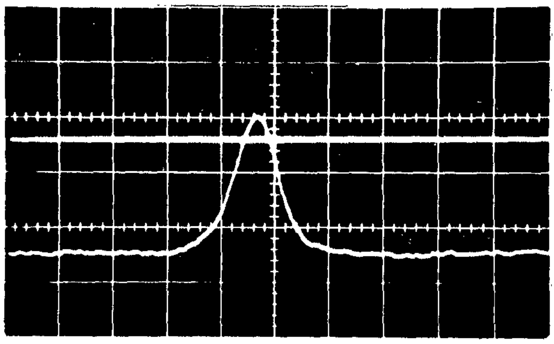

Upper Trace: Input Signal
Vertical Gain 0.05 volts/cm
Horizontal Sweep Speed 50 μsec/cm

Lower Trace: Output Signal From Antenna Port
Vertical Gain 0.005 volts/cm
Horizontal Sweep Speed 50 μsec/cm

Figure 16. Burst No. 10, Waveforms of Input and Output Signals from a Circulator Operating at 5.6 Gc

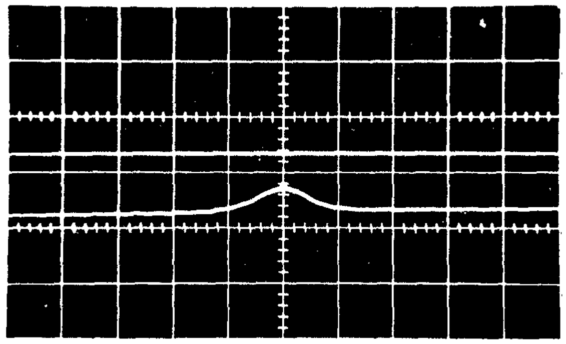

Upper Trace: VSWR Signal
Vertical Gain 0.05 volts/cm
Horizontal Sweep Speed 50 μsec/cm

Lower Trace: Output Signal from Receiver Port
Vertical Gain 0.005 volts/cm
Horizontal Sweep Speed 50 μsec/cm

Figure 17. Burst No. 4, Waveforms of VSWR and Output Signals from a Circulator Operating at 5.6 Gc

will be placed. Figure 17 (lower trace) is a photograph of the change in signal level detected during the fourth burst from the receiver port of a circulator operating at 5.6 Gc.

A rather interesting result[4] of the September, 1962 series of tests was the fact that the values of isolation between the transmitter and receiver ports of the test circulator had apparently increased due to the exposure to the radiation. This apparent effect was very carefully monitored prior to and after the January, 1963 series of tests. The results of these measurements for circulator Model D 52C1, Serial No. 70 are shown in Figure 18. It is evident that no significant increase in isolation occurred to the circulator which was exposed during bursts 1 through 16. This would indicate that the results obtained earlier were somewhat equivocal and that exposure to radiation does not cause a permanent change in the electromagnetic propagation properties of the garnet, such as an increase in the isolation between the transmitter and receiver ports of the three-port Y-junction circulator.

Analysis of the data in Figures 16 and 17 and all other data for the circulator tests will be discussed and tabulated in a later section of this report.

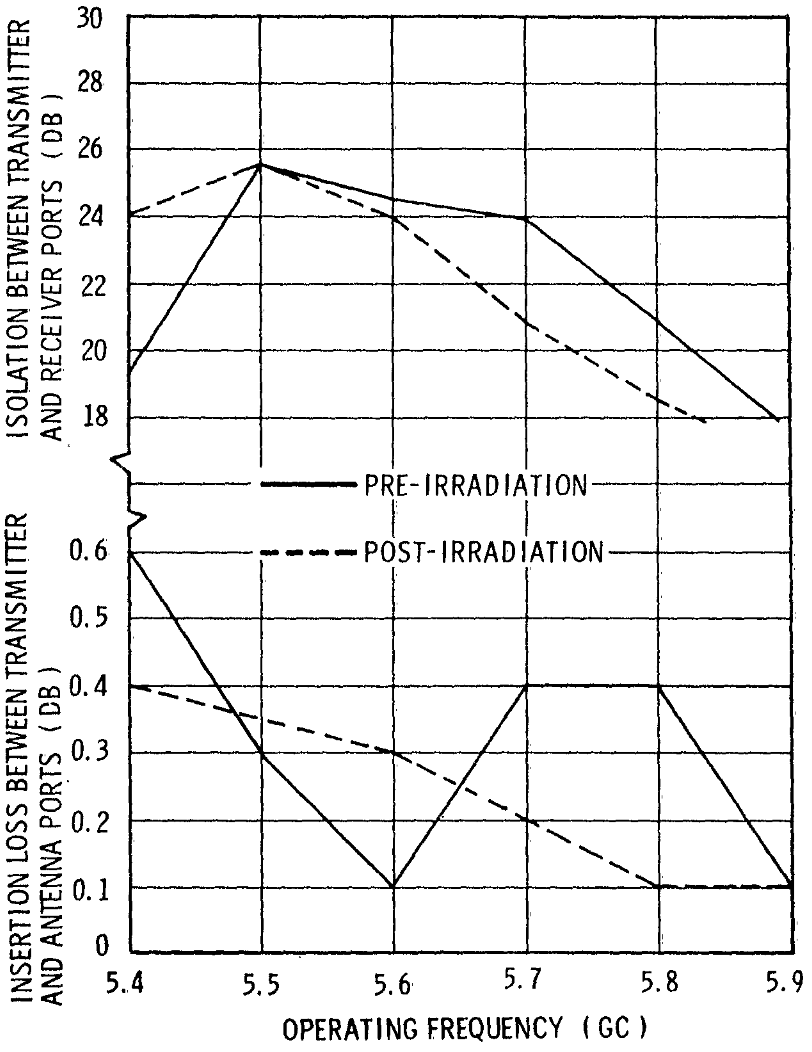

Figure 18. Post- and Pre-Irradiation Characteristics of Test Circulator, Model D52C1, Serial No. 70

Limiters. The gyromagnetic coupling limiter tests were performed using a single limiter, and a circulator-limiter duplexer (the latter tests will be discussed in the section dealing with configurations involving more than one component) operating at a frequency of 5.6 Gc and at power levels of 125 milliwatts and above.

Figure 19 is a representative photograph of the limiter data obtained during the seventh and fifteenth bursts. Figure 19 (lower trace) is a photograph of the change in signal level detected during the seventh burst from the output of a limiter operating at 5.6 Gc.

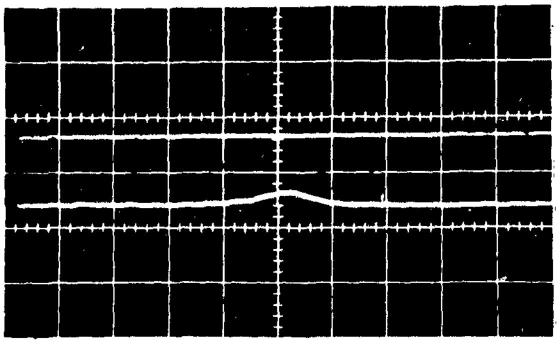

Upper Trace: Input Signal
Vertical Gain 0.05 volts/cm
Horizontal Sweep Speed 50 μsec/cm

Lower Trace: Output Signal
Vertical Gain 0.02 volts/cm
Horizontal Sweep Speed 50 μsec/cm

Figure 19. Burst No. 7, Waveforms of Input and Output Signals of Limiter Tuned to 5.6 Gc

The question of whether the values of insertion loss of the limiter were changed due to irradiation (as discussed in the preceding section) suggested that careful measurements of the insertion loss of the limiter also be made prior to and after exposure. The results of these measurements are shown in Figure 20. There is no apparent effect of the radiation on the insertion loss of the limiter.

Analysis of the data in Figure 19 and all other data for the limiter tests will be discussed and tabulated in a later section of this report.

Isolators. As noted in the last quarterly report[5] the C-band internal magnet coaxial isolator is not an integral component of the specific ferrite duplexer under investigation in this study; however, isolators of the type tested are ferrite devices which operate on the same non-reciprocity principle as do the circulators. Thus the isolator is a logical device to test, in order to discriminate between radiation effects on ferrite devices in general and radiation effects on the ferrite circulators in particular.

The internal magnet coaxial isolator tests were performed using a single isolator operating at a frequency of 5.6 Gc and at power levels of 125 milliwatts and above.

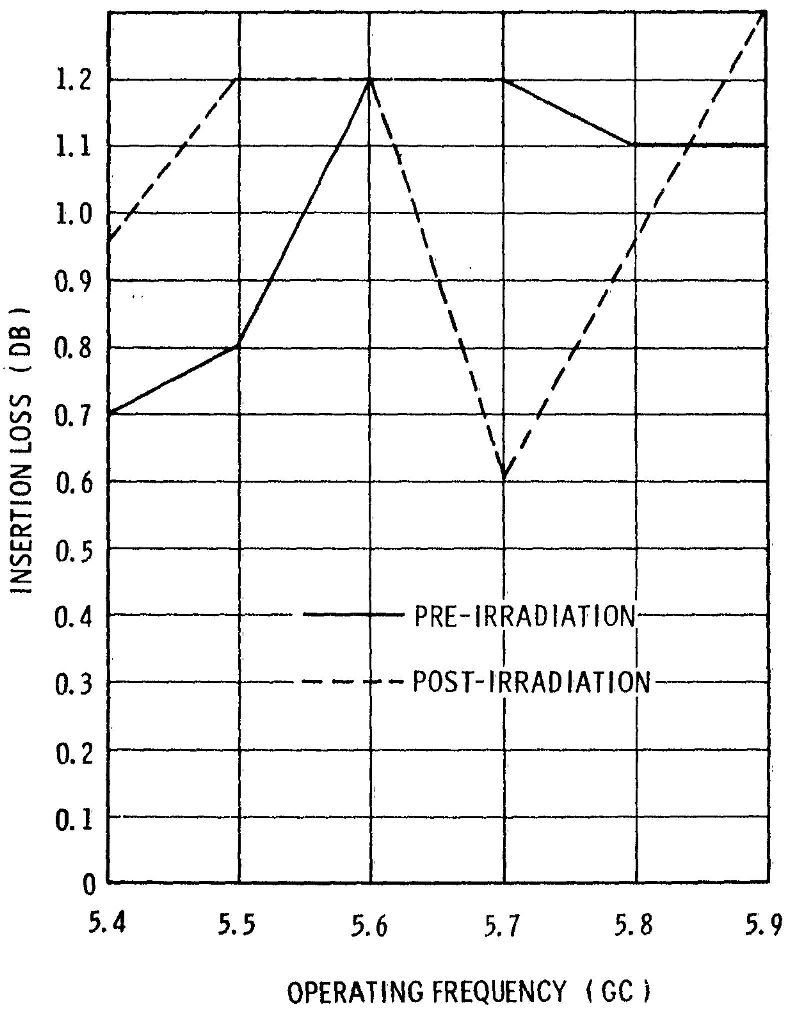

Figure 20. Post- and Pre-Irradiation Characteristics of the Test Limiter, Laboratory Model

Figure 21 is a representative photograph of the limiter data obtained during the sixth through the ninth bursts. Figure 21 (lower trace) is a photograph of the change in signal level detected during the sixth burst from the output of an isolator operating in the forward direction at 5.6 Cc. Tests were also made with the isolator operating in the reverse direction to determine whether the isolation characteristics would be changed.

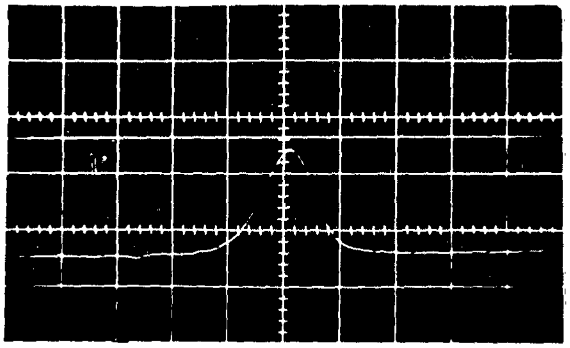

Upper Trace: Input Signal
Vertical Gain 0.05 volts/cm
Horizontal Sweep Speed 50 μsec/cm

Lower Trace: Output Signal (Insertion Loss)
Vertical Gain 0.005 volts/cm
Horizontal Sweep Speed 50 μsec/cm

Figure 21. Burst No. 6, Waveforms of Input and Output Signals From an Isolator Operating in the Forward Direction at a Frequency of 5.6 Gc

Measurements of the insertion loss and isolation of the test isolator (Model D44C7, Serial No. 204) were also made prior to and after the radiation exposure. The results of these measurements are shown in Figure 22. There is no consistent apparent effect of the radiation on the insertion loss or the isolation of the test isolator.

Analysis of the data in Figure 21, and all other data for the isolator tests, will be discussed and tabulated in a later section of this report.

<u>Configurations Involving More Than One Component</u>. Tests involving configurations of more than one component and/or the use of a signal source (front end) inside the KIVA were conducted for three reasons:

- To test certain components at powers above one watt,
- To obtain more accurate measurements of changes in the VSWR signal, and
- To test a circulator-limiter duplexer.

Powers to the components of greater than one watt were achieved by placing a front end usually made up of a klystron, klystron blower, waveguide variable attenuator, waveguide-to-coax adapter and isolator on the test platform behind the test component. Since it was considered quite probable that the radiation environment would affect the normal operation of the front end components and this

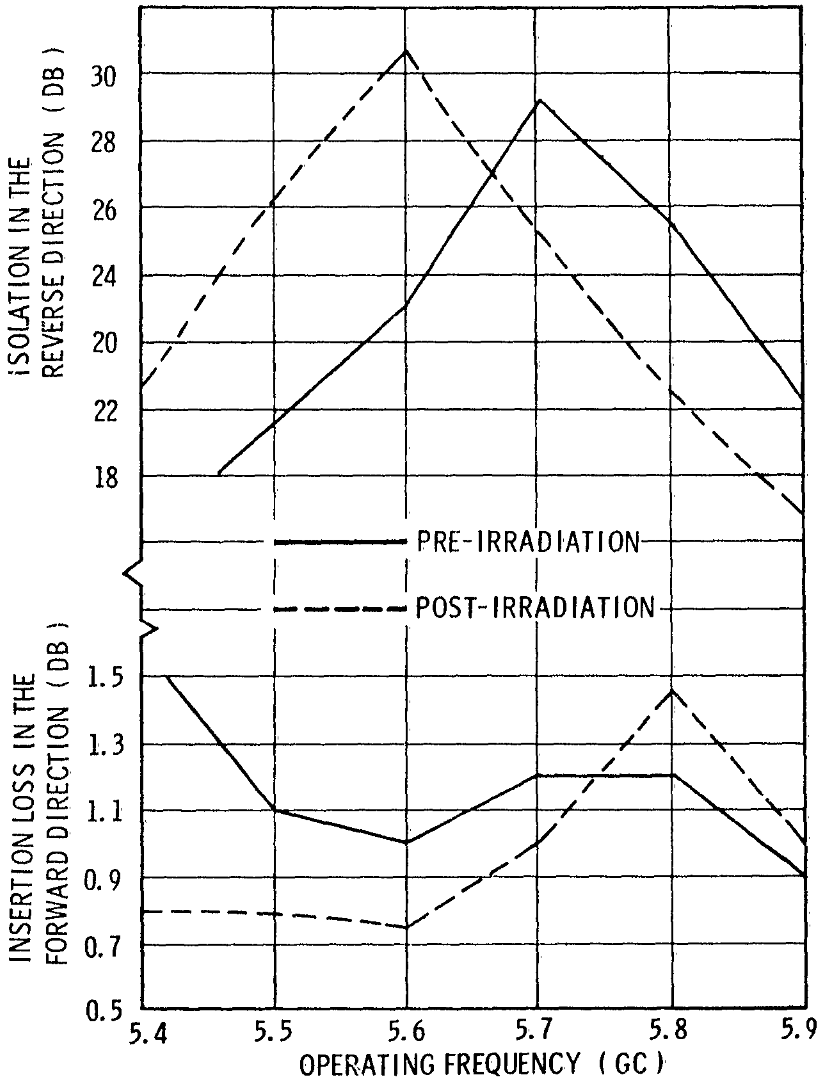

Figure 22. Post- and Pre-Irradiation Characteristics of Test Isolator, Model D44C7, Serial No. 204

effect would show up superimposed on the effects in the test specimen, "dummy" tests were performed in order to determine the magnitude of the front end effects. A more sensitive measurement of reflected power (VSWR) is possible if a three-port circulator is placed immediately in front of the component under test. In the conventional measuring scheme (see Figure 1) the magnitude of the VSWR signal would be decreased by approximately 30 db (due to having to travel 55 feet into the KIVA and 55 feet back out of the KIVA in RG 5 B/U cable) from the input power level at the klystron. The VSWR signal, attenuated 30 db, is competing for detection against a leakage signal from the transmitter port which may only be attenuated 20 db due to the isolation between the receiver and transmitter ports. This problem may be circumvented by placing the circulator immediately adjacent to the component and thus eliminating a 55 foot portion of the 110 foot cable run into the KIVA. The circulator-limiter duplexer was tested to determine whether the effects evidenced in individual components would be combined in any consistently additive manner when two components were joined together to make a single device.

Individual tests involving the front end in the KIVA or multi-component configurations were almost all

prototypes. The test schemes were similar in content to those previously discussed. A written discussion of each individual test would be somewhat lengthy and unwarranted for interpretation of the data and thus will not be given.

Figures 23 through 25 are representative photographs of the data obtained with the front end in the KIVA and configurations involving more than one component. These experiments were performed during the eighth through the sixteen bursts. Figure 23 (lower trace) is a photograph of the change in signal level detected during the ninth burst from the output of the limiter (limiter placed on receiver port of circulator to form circulator-limiter duplexer) operating at 5.6 Gc. In this configuration the power was supplied to the transmitter port of the circulator; the receiver port of the circulator was connected to the input port of the limiter; the received (coupled through or reflected) signal was detected at the output port of the limiter and the circulator insertion loss (transmitted signal) was measured at the antenna port of the circulator. Figure 24 (lower trace) is a photograph of the change in signal level detected during the twelfth burst from the antenna port of the primary circulator in a two circulator tandem configuration operating at 5.4 Gc. In this configuration the power was supplied to the transmitter port of the secondary circulator, the antenna port of the secondary circulator was connected to the transmitter port of the primary circulator, insertion loss and

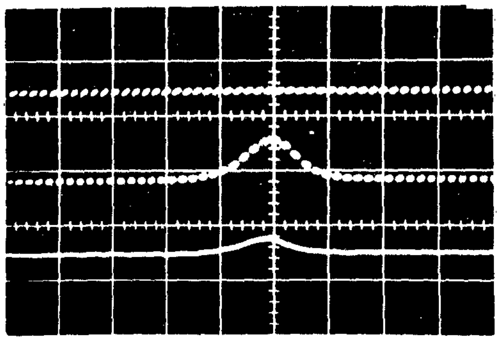

Upper Trace: Input Signal to Circulator-Limiter Duplexer
Vertical Gain 0.05 volts/cm
Horizontal Sweep Speed 50 μsec/cm

Middle Trace: Output Signal from Circulator (Transmitted Signal)
Vertical Gain 0.05 volts/cm
Horizontal Sweep Speed 50 μsec/cm

Lower Trace: Output Signal from Limiter of Circulator-Limiter Duplexer (Received Signal)
Vertical Gain 0.02 volts/cm
Horizontal Sweep Speed 50 μsec/cm

Figure 23. Burst No. 9, Waveforms of Input and Output Signals of Circulator-Limiter Duplexer and Output Signal from Single Circulator Operating at 5.6 Gc

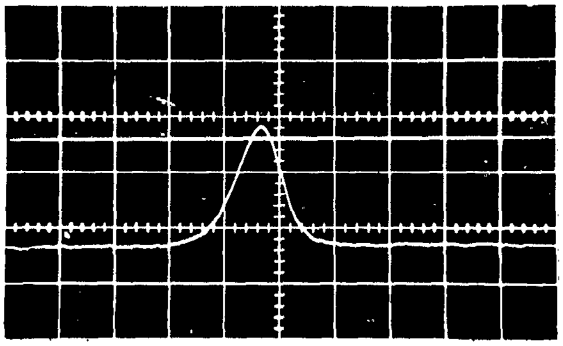

Upper Trace: Input Signal to Tandem Circulators
Vertical Gain 0.05 volts/cm
Horizontal Sweep Speed 50 μsec/cm

Lower Trace: Output Signal from Antenna Port of Primary Circulator
Vertical Gain 0.005 volts/cm
Horizontal Sweep Speed 50 μsec/cm

Figure 24. Burst No. 12, Waveforms of Input and Output Signals of Tandem Circulators Operating at 5.4 Gc

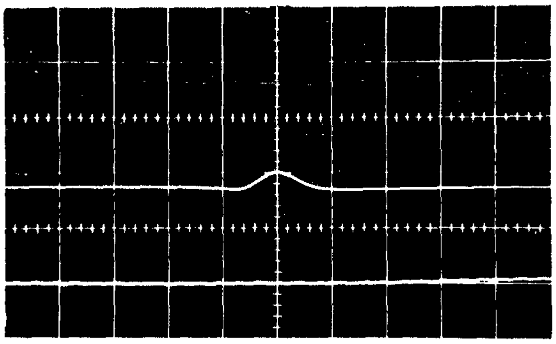

Upper Trace: Output Signal from Irradiated Front End
Vertical Gain 0.05 volts/cm
Horizontal Sweep Speed 50 μsec/cm

Lower Trace: Output Signal from Receiver Port of Signal Circulator
Vertical Gain 0.005 volts/cm
Horizontal Sweep Speed 50 μsec/cm

Figure 25. Burst No. 11, Waveforms of Output Signals from Irradiated Front End and Receiver Port of Single Circulator Operating at 5.6 Gc

isolation signals were detected at the antenna and receiver ports of the primary circulator, respectively, and the VSWR signal was detected at the receiver port of the secondary circulator.

Figure 25 (upper trace) is a photograph of the change in signal level detected during the eleventh burst from the output of the isolator on the irradiated front end. The front end inside the KIVA consisted of a klystron, klystron blower, waveguide variable attenuator, waveguide-to-coax adapter and an isolator.

Analysis of the data in Figures 23 through 25 and all other data for the front end in the KIVA and configurations involving more than one component will be discussed and tabulated in a later section of this report.

4.1.5 DC Voltage Experiments

Components tested in the high voltage dc experiments included the circulator, limiter, isolator, assorted half-potted* and unpotted connectors, waveguide elements and open-ended pieces of RG 58 C/U and RG 5 B/U cable. The experimental configuration for these tests has been described and pictured in a previous section (Section 4.1.2, Figure 7) and will not be covered here.

---

* The potting compound used in these experiments was Dow Corning Sylgard 183. The dielectric constant of this resin at C-band frequencies is greater than 3.00. Thus when used in microwave experiments it is not a suitable replacement for air, but for the dc experiments there were, of course, no problems of this nature.

Figures 26 and 27 are representative photographs of the data obtained from the dc experiments. These type experiments were performed during all sixteen bursts. Figure 26 (upper trace) is a photograph of the change in signal level detected during the sixth burst with 460 volts dc applied to the input port of a limiter; also shown (lower trace) is a photograph of the change in signal level detected during the sixth burst with 430 volts dc applied to an aluminum air filled waveguide element. A positive polarity was used in both experiments -- this means that the electron flow was from the outside sheath of the RG 58 C/U cable to the center conductor. Figure 27 (upper trace) is a photograph of the change in signal level detected during the fifteenth burst with 460 volts dc applied to a short piece of open-ended RG 5 B/U cable; also shown (lower trace) is a photograph of the change in signal level detected during the fifteenth burst with 430 volts dc applied to the input port of an isolator. A negative polarity was used in both experiments -- this means that the electron flow was from the inner conductor to the outer sheath of the RG 58 C/U cable.

Analysis of the data in Figure 26 and Figure 27, and all other data for the dc experiments, will be discussed and tabulated in a later section of this report.

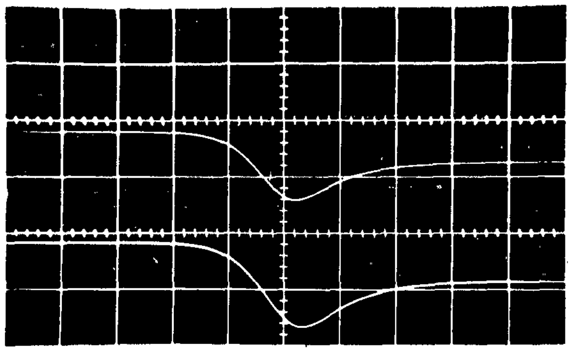

Upper Trace: Limiter with 460 volts dc Applied with Positive Polarity
Vertical Sensitivity 0.20 volts/cm
Horizontal Sweep Speed 50 μsec/cm

Lower Trace: Air Filled Aluminum Waveguide with 430 volts dc Applied with Positive Polarity
Vertical Sensitivity 0.20 volts/cm
Horizontal Sweep Speed 50 μsec/cm

Figure 26. Burst No. 6, Signal Response from Limiter and Aluminum Waveguide to 460 and 430 volts dc Applied with Positive Polarity

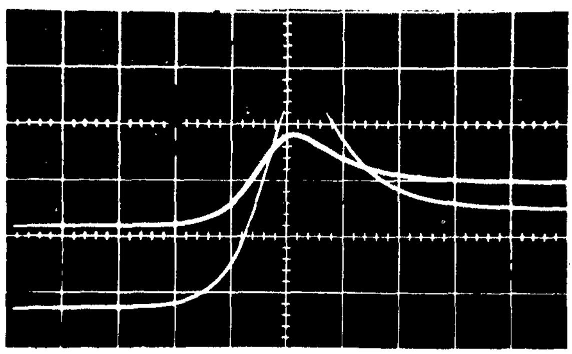

Upper Trace: Open Ended Piece of RG 5 B/U Cable with 460 volts dc Applied with Negative Polarity
Vertical Sensitivity 0.05 volts/cm
Horizontal Sweep Speed 50 μsec/cm

Lower Trace: Isolator with 430 volts dc Applied with Negative Polarity
Vertical Sensitivity 0.10 volts/cm
Horizontal Sweep Speed 50 μsec/cm

Figure 27. Burst No. 15, Signal Response from Open Ended Piece of RG 5 B/U Cable and Isolator to 460 and 430 volts dc Applied with Negative Polarity

4.1.6 Component Activation

After the series of experiments was completed, the health physics personnel at the SPRF survey-monitored all equipment and components that had been inside the KIVA during one or more bursts. The results of these surveys indicated that the limiters, the circulators, the aluminum mounting platforms, the waveguides, the klystron, waveguide attenuator and adapters had been activated to levels ranging from 10 to 50 mr/hour. The activity was predominantly made up of electrons and was considered to be of short-lived duration. All other components which were exposed to a number of bursts were found to be somewhat β active, 1-2 mr/hour. This activity was also of short-lived duration and not considered significant.

4.2 ANALYSIS OF DATA AND RESULTS

4.2.1 Calibration Procedures

Correlations of the millivolt deflections observed on the oscilloscopes to db changes in the operating characteristics of the components were obtained by much the same methods as those used during the September series of experiments.[6] These methods made use of calibrated variable attenuators (PRD Model 173D) which were inserted in the circuit front ends immediately behind the klystrons (see Figure 1). Attenuations (as measured on both a VSWR meter,

Sperry Microline Model 29A1 and a power meter, Sperry Model 31A1) of 0, 0.5, 1.0, 1.5, 2.0 and 3.0 db were introduced into each test circuit by means of the calibrated attenuators. A photograph of all these six cw signal levels representative of the six different known attenuations was obtained for both preamplifiers of each scope. The preamplifier vertical sensitivities were recorded and correlations between millivolts in deflection of the cw signals due to a burst of nuclear radiation and db power level changes within the circuits were established.

The settings on the calibrated variable attenuators for 0.5, 1.0, 1.5, 2.0 and 3.0 db attenuations were determined by measuring power outputs at the positions normally occupied by the crystal detectors used to monitor the input signals of the three test set ups. These settings were determined for 1000 cycle square wave modulation operation of the klystrons. It was later felt that the crystal detectors and VSWR meter at the monitor signal outputs were being driven, powerwise, into a region above square-law operation*. Since the VSWR meter and crystal detector

---

* Square-law detection implies that the output signal is proportional to the square of the amplitude of the input signal. This type behavior is illustrated analytically by a Taylor expansion of the output current as a function of the input voltage terminating in the square term. It can be shown that any rectifier will function as a square-law detector when the applied signal is sufficiently small.[7]

were used at the same location in the circuit, and the VSWR meter is a square-law device, the crystal detector should also have been operated as a square-law device for the calibration. Crystal detector operation, at powers out of the square-law region, degrades behavior into a linear response. For this reason a recalibration with sufficient padding ahead of the crystal detector, to guarantee square-law operation, was required. These recalibrations were performed, and the data properly corrected.

As an illustration of these effects, the results of the recalibration for the third test set up are shown in Table 3 wherein they are associated with the original attenuations of 0, 0.5, 1.0, 1.5, 2.0 and 3.0 db.

TABLE 3. RECALIBRATION OF ATTENUATIONS INTRODUCED INTO TEST SET-UP NUMBER 3

Attenuations For Power Above Square-Law Behavior Region, db	Corresponding Attenuations For Power Within Square-Law Behavior Region, db
0	0
0.5	0.85
1.0	1.9
1.5	2.9
2.0	3.7
3.0	5.4

Figure 28 is typical of the results of the calibrations. This particular photograph was taken on oscilloscope number four (inputs 7 and 8) prior to the first radiation burst. The vertical sensitivity for both preamplifiers was 0.05 volt/cm. Five (the dc experiments were not calibrated in this manner) such photographs were obtained whenever circuit (cable or component) changes were made between succeeding bursts. The ten such sets of data for bursts one and two are plotted in Figure 29. Curves such as those shown in Figure 29 were used to derive quantitative values for the changes in power levels at the test specimens for all sixteen bursts.

The following sections of the report contain tabulations of the calibrations of all data in which a signal level change was detected.

4.2.2 Waveguide Results

All waveguide data in which a change in signal level was detected have been analyzed by the use of calibration curves similar to those described above. The results of these analyses are presented in Table 4. All columns in the table except those discussed in the remainder of this paragraph are considered to be self-explanatory. The fourth column lists the input number which was used for the specified signal during the burst indicated. Inputs 1 and 2

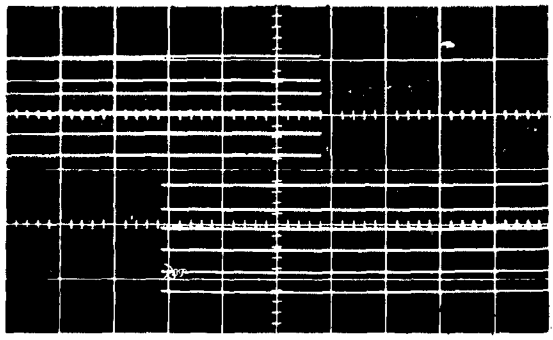

Upper Signals: VSWR from a Circulator
Vertical Gain 0.05 volts/cm
Horizontal Sweep Speed 50 μsec/cm

Lower Signals: Output from Receiver Port of Circulator
Vertical Gain 0.05 volts/cm
Horizontal Sweep Speed 50 μsec/cm

Figure 28. Signal Level Changes (in Millivolts) Caused by Insertion of 0, 0.85, 1.9, 2.9, 3.7 and 5.4 db Attenuation Steps Into Test Circuit

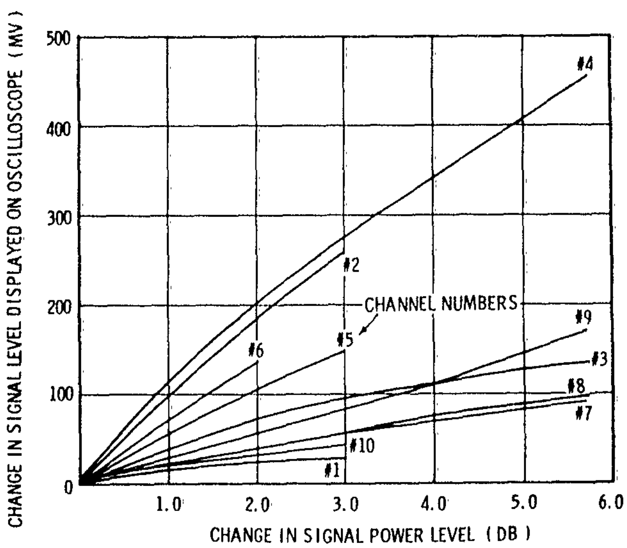

Figure 29. Burst No. 1, Calibration Curves Relating Millivolt Signal Level Changes to db Power Level Changes

Table 4. Results of Radiation Environment Tests of Brass and Aluminum Waveguide Elements and "Butted Together" Waveguide-to-Coax Adapters (Bursts 1 - 6)

1 Iden. No.	2 Burst No.	3 Burst Size °C	4 Input No.	5 Type of Test Specimen	6 Dielectric	7 Signal	8 Crystal Detector No.	9 Crystal Sensitivity mv/db	10 Vertical Gain mv/cm	11 Magnitude of Effect mv	12 Magnitude of Effect DB
1	1	100.7	10	Brass Waveguide	Air	VSWR	6	25	50	4	0.160
2	2	107.0	2	Brass Waveguide	Air	Output	1	100	10	33.5	0.335
3	2	107.0	4	Aluminum Waveguide	Air	Output	2	116	10	26.0	0.224
4	3	108.6	2	Brass Waveguide	Air	Output	1	84	10	31.0	0.369
5	3	108.6	4	Aluminum Waveguide	Air	Output	2	85	10	26.5	0.312
6	4	108.0	2	Brass Waveguide	Low Density Styrofoam	Output*	1	76	100	~ 70	0.922
7	4	108.0	4	Aluminum Waveguide	High Density Styrofoam	Output	2	64	10	5.8	0.091
8	5	109.7	2	Brass Waveguide	High Density Styrofoam	Output	1	60	10	6.2	0.103
9	5	109.7	4	Aluminum Waveguide	Low Density Styrofoam	Output	2	91	20	64	0.703
10	5	109.7	10	Brass Waveguide	High Density Styrofoam	VSWR	6	17	5	0.2	0.012
11	6	108.0	2	Two Aluminum Waveguide-to-Coax Adapters "Butted Together"	Air	Output	1	69	5	13.5	0.196
12	6	108.0	10	Two Aluminum Waveguide-to-Coax Adapters "Butted Together"	Air	VSWR	6	17	5	0.6	0.035

*This pulse was not photographed directly due to incorrect vertical gain settings on the preamplifier. The photograph was obtained from a playback of the magnetic tape.

were applied to preamplifiers 1 and 2 of oscilloscope number 1, inputs 3 and 4 were applied to preamplifiers 1 and 2 of oscilloscope number 2, etc. The seventh column identifies each of the signals. In some instances (those denoted by an asterisk) the change in signal level was so large that the pulse went off scale for the vertical gain settings used on the oscilloscope at the time of the burst. Well defined photographs of these pulses were later obtained by playing back the magnetic tape and photographing the playback signal on an oscilloscope on which a less sensitive vertical gain setting was used. The ninth column presents the crystal detector sensitivity which is defined as the number of millivolts change in the vertical position of the trace per db of attenuation inserted into the circuit. The crystal sensitivities were determined from the calibration curves previously described. Column 10 indicates the vertical sensitivity settings on the preamplifiers associated with each set of data. Column 11 presents the magnitude of the radiation effect in the waveguide in millivolts -- these values were obtained directly from the oscilloscope photographs for each burst. The last column gives the magnitude of the radiation effect in terms of db, namely, magnitude of effect in db (value in column 12)

$$= \frac{\text{Magnitude of effect in millivolts (value in column 11)}}{\text{Crystal sensitivity in millivolts/db (value in column 9)}}.$$

The following conclusions concerning the waveguide data were drawn from a review of the values presented in the 12th column of Table 4.

- The data from bursts 2 and 3 (identification numbers 2, 3, 4 and 5) indicate that the increase in the magnitude of the attenuations of the brass and aluminum waveguide elements due to the radiation bursts was 0.352 db and 0.268 db, respectively, which were superimposed on inherent per foot attenuations of 0.015 db[8] and 0.012 db[9], respectively. Since one foot waveguide sections were exposed, <u>the radiation caused a 2350 per cent transient increase in attenuation in the brass waveguide (air dielectric) and a 2230 per cent transient increase in attenuation in the aluminum waveguide (air dielectric)</u>.

- The data from bursts 4 and 5 (identification numbers 6 and 9) indicate that the increase in the magnitude of the attenuations of the brass and aluminum waveguide elements (loaded with low density Styrofoam) due to the radiation burst was 0.922 db and 0.703 db, respectively, which were superimposed on inherent per foot attenuations of approximately 0.015 db and 0.012 db, respectively. Since one foot waveguide sections were exposed, <u>the radiation burst caused a 6150 per cent transient increase in attenuation in the brass waveguide (low density Styrofoam dielectric filled) and a 5860 per cent transient increase in attenuation in the aluminum waveguide (low density Styrofoam dielectric filled)</u>.

- The data from bursts 4 and 5 (identification numbers 7 and 8) indicate that the increase in the magnitude of the attenuations of the brass and aluminum waveguide elements (loaded with high density Styrofoam) due to the radiation burst was

> 0.103 db and 0.091 db, respectively, which were superimposed on inherent per foot attenuations of approximately 0.015 db and 0.012 db, respectively. Since one foot waveguide sections were exposed, <u>the radiation burst caused a 687 per cent transient increase in attenuation in the brass waveguide (high density Styrofoam dielectric filled) and a 758 per cent transient increase in attenuation in the aluminum waveguide (high density Styrofoam dielectric filled)</u>.

The data from burst number 6 (identification numbers 11 and 12) is not thought to be an acceptable quantitative measure of the radiation effects in the coax-to-waveguide adapters. There is some doubt that the electromagnetic wave (signal) was satisfactorially "launched" from the probe in the first waveguide since the length of cavity available between the "launching" and "receiving" probes was very short (~9.84 cm for a signal wavelength of ~5.36 cm).

4.2.3 <u>Circulator Results</u>

Table 5 presents the results of the analyses of all circulator data in which a change in signal level was detected. As previously noted, one circulator (Serial No. 70) was irradiated in all bursts. During bursts 8 and 9 this circulator was connected in tandem with a second circulator and this data will be reported in a later section of the report.

The following general conclusions concerning C-band coaxial ferrite Y-junction circulator data were drawn from an examination of the values presented in column 13 of Table 5.

- The data from bursts 1, 3-7 and 10-16 (identification numbers 1, 3, 5, 7, 9, 11, 14-19 and 21) indicate that the average increase in the magnitude of the insertion loss between the transmitter and antenna ports of the circulator due to the radiation burst was 0.04 db which was superimposed on a maximum inherent insertion loss of 0.5 db. Thus, the radiation caused a 8 per cent transient increase in insertion loss in the circulator.

The datum from burst number 10 (identification number 13) was neglected since it is a factor 5 greater than the average value and no justifiable reason for accepting this discrepancy is readily apparent.

- The data from bursts 1, 3-7 and 16 (identification numbers 2, 4, 6, 8, 10, 12 and 22) indicate that the average increase in the magnitude of the isolation between the transmitter and receiver ports of the circulator due to the radiation burst was 0.09 db which was superimposed on an inherent minimum isolation of 20 db. Thus, the radiation appeared to cause a 0.5 per cent transient increase in isolation in the circulator.

With reference to this apparent increase in insertion loss and isolation, it should be noted that the magnitude of these effects are comparable to the magnitude of the radiation effects previously noted in type N connectors[10]. Thus, the apparent increase

Table 5. Results of Radiation Environment Tests of C-Band Coaxial Ferrite Y-Junction Circulators (Bursts 1 through 16) (Sheet 1 of 2)

1 Iden. No.	2 Burst No.	3 Burst Size °C	4 Input No.	5 Component	6 Frequency, Gc	7 Distance from Reactor, Inches	8 Signal	9 Crystal Detector No.	10 Crystal Sensitivity mv/db	11 Vertical Gain mv/cm	12 Magnitude of Effect, mv	13 Magnitude of Effect DB
1	1	100.7	6	Circulator	5.6	3.5	Output from Antenna Port	4	68	5	2.3	0.034
2	1	100.7	8	Circulator	5.6	3.5	Output from Receiver Port	3	20	5	1.9	0.095
3	3	108.6	6	Circulator	5.6	3.5	Output from Antenna Port	4	65	5	3.4	0.052
4	3	108.6	8	Circulator	5.6	3.5	Output from Receiver Port	3	39	5	2.1	0.054
5	4	108.0	6	Circulator	5.6	3.5	Output from Antenna Port	4	58	5	3.3	0.057
6	4	108.0	8	Circulator	5.6	3.5	Output from Receiver Port	3	20	5	2.3	0.115
7	5	109.7	6	Circulator	5.6	3.5	Output from Antenna Port	4	76	5	3.3	0.043
8	5	109.7	8	Circulator	5.6	3.5	Output from Receiver Port	3	20	5	1.9	0.095
9	6	108.0	6	Circulator	5.6	3.5	Output from Antenna Port	4	64	5	3.1	0.049
10	6	108.0	8	Circulator	5.6	3.5	Output from Receiver Port	3	20	5	2.0	0.100
11	7	108.5	6	Circulator	5.6	3.5	Output from Antenna Port	4	71	5	3.3	0.047
12	7	108.5	8	Circulator	5.6	3.5	Output from Receiver Port	3	28	5	2.1	0.075
13	10	114.0	2	Circulator	5.6	2.5	Output from Antenna Port	1	60	5	12.5	0.208
14	11	109.5	2	Circulator	5.6	30.0	Output from Antenna Port	1	116	5	2.1	0.018
15	12	112.3	2	Circulator	5.6	54.5	Output from Antenna Port	1	106	5	1.9	0.018

Table 5. Results of Radiation Environment Tests of C-Band Coaxial Ferrite Y-Junction Circulators (Bursts 1 through 16) (Sheet 2 of 2)

1 Iden No.	2 Burst No.	3 Burst Size °C	4 Input No.	5 Component	6 Frequency, Gc	7 Distance from Reactor, Inches	8 Signal	9 Crystal Detector No.	10 Crystal Sensitivity mv/db	11 Vertical Gain mv/cm	12 Magnitude of Effect, mv	13 Magnitude of Effect DB
16	13	107.5	4	Circulator	5.4	4.0	Output from Antenna Port	3	180	5	8.7	0.048
17	14	107.2	2	Circulator	5.6	75.0	Output from Antenna Port	1	86	5	1.0	0.012
18	14	107.2	4	Circulator	5.4	4.0	Output from Antenna Port	3	180	5	8.8	0.049
19	15	106.0	4	Circulator	5.6	3.5	Output from Antenna Port	3	180	5	8.0	0.044
20	15	106.0	6	Circulator	5.6	3.5	Output from Receiver Port	4	2.2*	5	0.2	0.091*
21	16	107.5	4	Circulator	5.9	3.5	Output from Antenna Port	3	130	5	7.1	0.055
22	16	107.5	6	Circulator	5.9	3.5	Output from Receiver Port	4	14	5	0.8	0.057

*Poor calibration sensitivity

in insertion loss and isolation noted above may be caused by a decrease in signal level due to radiation effects in the type N connectors making up the external transmitter, antenna, and receiver ports of the circulator.

4.2.4 Limiter Results

Table 6 presents the results of all the gyromagnetic coupling limiter data in which a change in signal level was detected. Very little data were obtained for single operating limiters during this series of experiments. Rather, attention was focused on studying a circulator-limiter duplexer and the data from these studies will be reported in a later section of this report.

The following general conclusions are drawn from a consideration of the values presented in column 13 of Table 6.

- The datum from burst 7 (identification number 1) substantiates[11] the fact that the average increase in the magnitude of the insertion loss of the limiter due to the radiation burst was 0.10 db which was superimposed on an inherent insertion loss of 1.2 db. Thus the radiation caused a 8.3 per cent transient increase in the insertion loss in the limiter.

- The datum from burst 15 (identification number 3), although hardly conclusive due to poor calibration sensitivity, indicates that for a power of 0.8 watts incident to the limiter the increase in the magnitude of the insertion loss in the limiter due to the radiation burst was 1.0 db which was superimposed on an inherent insertion loss of 1.2 db. Thus for a power level of 0.8 watts the radiation caused a 83 per cent transient increase in the insertion loss in the limiter.

Table 6. Results of Radiation Environment Tests of C-Band Gyromagnetic Coupling Limiter (Bursts 7 & 15)

1 Iden. No.	2 Burst No.	3 Burst Size °C	4 Input No.	5 Component	6 Frequency Gc	7 Distance from Reactor, Inches	8 Signal	9 Cyrstal Detector No.	10 Crystal Sensitivity mv/db	11 Vertical Gain mv/cm	12 Magnitude of Effect mv	13 Magnitude of Effect DB
1	7	108.5	2	Limiter tuned to 5.6 Gc	5.6	1.5	Return signal	1	48	20	5	0.104
2	7	108.5	10	Limiter tuned to 5.6 Gc	5.6	1.5	VSWR	6	13*	5	0.25	0.019
3	15	106.0	10	Limiter not tuned to 5.6 Gc**	5.6	3.0	Return signal	6	19*	5	20	1.052

*Poor calibration sensitivity

**This limiter was supplied by a front end inside the KIVA. Power input of approximately 0.8 watts.

The latter conclusion should be considered as more qualitative than quantitative but the idea that the radiation effects become more pronounced at higher powers is certainly probable.

4.2.5 Isolator Results

Table 7 presents the results of the analyses of all internal magnet coaxial isolator data in which a change in signal level was detected.

The following general conclusions are drawn from a consideration of the values presented in column 13 of Table 7.

- The datum from burst 6 (identification number 1) indicates that the increase in the magnitude of the insertion loss in the isolator due to the radiation burst was 0.1 db which was superimposed on an inherent insertion loss of 0.9 db. Thus the radiation caused an 11 per cent transient increase in the insertion loss of the isolator.

- The datum from burst 7 (identification number 2) indicates that the increase in the magnitude of the isolation of the isolator (operating in the reverse direction) due to the radiation burst was 0.06 db which was superimposed on a minimum inherent isolation of 15 db. Thus the radiation caused a 0.4 per cent transient increase in the isolation of the isolator.

No attempt was made to interpret the data from the eighth and ninth radiation bursts (identification numbers 3 and 4) since the placement of the crystal detector inside the KIVA (at the isolator output) apparently had a serious effect on the normal operating response of the

Table 7. Results of Radiation Environment Tests of C-Band Internal Magnet Coaxial Isolator (Bursts 6 through 9)

1 Iden No.	2 Burst No.	3 Burst Size ^oC	4 Input No.	5 Component	6 Frequency Gc	7 Distance from Reactor, Inches	8 Signal	9 Crystal Detector No.	10 Crystal Sensitivity mv/db	11 Vertical Gain mv/cm	12 Magnitude of Effect mv	13 Magnitude of Effect DB
1	6	108.0	4	Isolator operating in forward direction	5.6	2.5	Return signal	2	95	5	9.2	0.097
2	7	108.5	4	Isolator operating in reverse direction	5.6	2.5	Return signal	2	13*	20	0.8	0.062
3	8	109.0	5	Isolator operating in reverse direction	5.6	2.5	Return signal	2**	25*	50	35***	1.400
4	9	109.5	5	Isolator operating in reverse direction	5.6	2.5	Return signal	2**	80	50	51***	0.637

*Poor calibration sensitivity due to reversed isolator

**Crystal detector inside KIVA

***This pulse was not photographed directly due to incorrect vertical gain setting on the preamplifier. The photograph was obtained from a playback of the magnetic tape.

crystal. The deterioration of the crystal response was verified after it had been removed from the KIVA by means of a sensitivity test. This effect was not unexpected and the possibility of crystal response deterioration in the presence of radiation was one of the items which was to be investigated during the January trip.

4.2.6 Results From Configurations Involving More Than One Component and Front End Inside KIVA Tests

Table 8 presents the results of the analyses of all data in which a change in signal level was detected for configurations involving more than one component and the front end inside the KIVA. These data are somewhat more difficult to analyze in a systematic fashion and thus, it is felt that the following conclusions should be regarded as more qualitative than quantitative even though quantitative values are presented therein.

The following general conclusions concerning configurations involving more than one component (viz., a circulator-limiter duplexer and two circulators in tandem) and the front end inside the KIVA were drawn from an examination of the values presented in column 13 of Table 8.

Circulator-Limiter Duplexer (Limiter Connected to Receiver Port of Circulator. Power Input to Transmitter Port)

- The data from bursts 8, 9, 15 and 16 (identification numbers 1, 6, 15 and 22) indicate that the average increase in the magnitude of the transmitter to receiver port isolation at the circulator plus the insertion loss of the limiter due to the radiation burst was 0.05 db. This increase was superimposed on a minimum inherent isolation of 20 db (circulator) and a maximum inherent insertion loss (limiter) of 1.0 db. Thus, the radiation caused a 0.2 per cent transient increase in signal attenuation between the input at the transmitter port of the circulator and the output port of the limiter.

The data from bursts 8, 9 and 16 (identification numbers 4, 7 and 23) were not analyzed because placement of the crystal detectors inside the KIVA degraded their performance and resulted in poor calibration and test sensitivity.

Tandem Circulators (Antenna Port of Secondary Circulator Connected to Transmitter Port of Primary Circulator. Power Input to Transmitter Port of Secondary Circulator)

- The data from bursts 10, 11 and 12 (identification numbers 11, 14 and 17) indicate that the average increase in the magnitude of the change in VSWR signal level from the primary circulator and/or the change in magnitude of the isolation of the secondary circulator due to the radiation burst was 0.05 db. This value is nearly equal to the increase in the isolation measured in the single circulator experiments (see Section 4.2.3). This fact suggests that there was no significant change in the VSWR signal level of the primary circulator but rather an increase in isolation between the transmitter and receiver ports of the secondary circulator.

Table 8. Results of Radiation Environment Tests of Front End Inside KIVA and Configurations Involving More Than One Component (Bursts 8 - 16) (Sheet 1 of 4)

1 Iden. No.	2 Burst No.	3 Burst Size °C	4 Input No.	5 Configuration under Test	6 Frequency Gc	7 Distance from Reactor Inches	8 Signal	9 Crystal Detector No.	10 Crystal Sensitivity mv/db	11 Vertical Gain mv/cm	12 Magnitude of Effect MV	13 Magnitude of Effect DB
1	8	109.0	2	Circulator with limiter tuned to 5.6 Gc attached to receiver port (Circulator-Limiter Duplexer)	5.6	1.5	Return signal from limiter	1	113	5	5.7	0.050
2	8	109.0	12	Circulator with limiter tuned to 5.6 Gc attached to receiver port (Circulator-Limiter Duplexer)	5.6	1.5	VSWR of component measured in trailer	6	20	5	0.6	0.030
3	8	109.0	3	Two circulators in tandem. Antenna port of secondary circulator connected to transmitter port of primary circulator	5.6	3.5	Output from receiver port of primary circulator	3**	112	50	50	0.446**
4	8	109.0	6	Circulator with limiter tuned to 5.6 Gc attached to receiver port (Circulator-Limiter Duplexer)	5.6	1.5	Insertion loss through circulator, antenna port	7**	10*	50	27.5	2.750**
5	8	109.0	10	Two circulators in tandem. Antenna port of secondary circulator connected to transmitter port of primary circulator	5.6	3.5	Output signal from receiver port of secondary circulator	8**	10*	5	8.5	0.850**
6	9	109.5	2	Circulator with limiter tuned to 5.6 Gc attached to receiver port (Circulator-Limiter Duplexer)	5.6	1.5	Return signal from limiter	1	94	20	5.6	0.060
7	9	109.5	6	Circulator with limiter tuned to 5.6 Gc attached to receiver port (Circulator-Limiter Duplexer)	5.6	1.5	Insertion loss through circulator, antenna port	7**	12*	50	17.5	1.458**
8	9	109.5	8	Two circulators in tandem. Antenna port of secondary circulator connected to transmitter port of primary circulator	5.6	3.5	Output signal from antenna port of primary circulator	4	62	5	2.9	0.047

Table 8. Results of Radiation Environment Tests of Front End Inside KIVA and Configurations Involving More Than One Component (Bursts 8 - 16) (Sheet 2 of 4)

1 Iden. No.	2 Burst No.	3 Burst Size °C	4 Input No.	5 Configuration under Test	6 Frequency Gc	7 Distance from Reactor Inches	8 Signal	9 Crystal Detector No.	10 Crystal Sensitivity mv/db	11 Vertical Gain mv/cm	12 Magnitude of Effect MV	13 Magnitude of Effect DB
9	9	109.5	10	Two circulators in tandem. Antenna port of secondary circulator connected to transmitter port of primary circulator	5.6	3.5	Output signal from receiver port of secondary circulator	8**	10*	5	10	1.000**
10	9	109.5	12	Circulator with limiter tuned to 5.6 Gc attached to receiver port (Circulator-Limiter Duplexer)	5.6	1.5	VSWR of component measured in trailer	6	9*	5	0.15	0.017
11	10	114.0	8	Two circulators in tandem. Antenna port of secondary circulator connected to transmitter port of primary circulator	5.6	4.0	VSWR measured at receiver port of secondary circulator	2	10*	5	0.40	0.040
12	10	114.0	10	Front end (klystron, waveguide attenuator, coax-to-waveguide adapter) inside KIVA	5.6	18.0	Output signal from front end	14	34	200	128***	3.765
13	11	109.5	4	Two circulators in tandem. Antenna port of secondary circulator connected to transmitter port of primary circulator	5.6	4.0	Return signal from antenna port of primary circulator	3	195	5	10	0.051
14	11	109.5	8	Two circulators in tandem. Antenna port of secondary circulator connected to transmitter port of primary circulator	5.6	4.0	VSWR signal from receiver port of secondary circulator	2	10*	5	0.5	0.050
15	11	109.5	9	Front end (klystron, waveguide attenuator, coax-to-waveguide adapter, isolator) inside KIVA	5.6	22.0	Output signal from front end	14	36	50	16	0.445

Table 8. Results of Radiation Environment Tests of Front End Inside KIVA and Configurations Involving More Than One Component (Bursts 8 - 16) (Sheet 3 of 4)

1 Iden. No.	2 Burst No.	3 Burst Size °C	4 Input No.	5 Configuration under Test	6 Frequency Gc	7 Distance from Reactor Inches	8 Signal	9 Crystal Detector No.	10 Crystal Sensitivity mv/db	11 Vertical Gain mv/cm	12 Magnitude of Effect MV	13 Magnitude of Effect DB
16	12	112.3	4	Two circulators in tandem. Antenna port of secondary circulator connected to transmitter port of primary circulator	5.4	4.0	Return signal from antenna port of primary circulator	3	180	5	10.8	0.060
17	12	112.3	8	Two circulators in tandem. Antenna port of secondary circulator connected to transmitter port of primary circulator	5.4	4.0	VSWR signal from receiver port of secondary circulator	2	16*	5	0.9	0.056
18	12	112.3	9	Front end (klystron, waveguide attenuator, coax-to-waveguide adapter) inside KIVA	5.6	22.0	Output signal from front end	14	50	50	4	0.080
19	13	107.5	9	Front end (klystron, waveguide attenuator, coax-to-waveguide adapter, isolator, circulator) inside KIVA	5.6	22.0	Output signal from antenna port of circulator	14	42	50	4	0.095
20	14	107.2	9	Front end (klystron, waveguide attenuator, coax-to-waveguide adapter, isolator, circulator) inside KIVA	5.6	22.0	Output signal from antenna port of circulator	14	42	50	6.0	0.143
21	15	106.0	2	Circulator with limiter tuned to 5.6 Gc attached to receiver port (Circulator-Limiter Duplexer)	5.6	0.75	Insertion loss through antenna port of circulator	1	74	5	3.0	0.041
22	16	107.5	2	Circulator with limiter tuned to 5.6 Gc attached to receiver port (Circulator-Limiter Duplexer)	5.6	0.75	Output signal from antenna port of circulator	1	76	5	5.0	0.066

Table 8. Results of Radiation Environment Tests of Front End Inside KIVA and Configurations Involving More Than One Component (Bursts 8 - 16) (Sheet 4 of 4)

1 Iden. No.	2 Burst No.	3 Burst Size	4 Input No.	5 Configuration under Test	6 Frequency Gc	7 Distance from Reactor Inches	8 Signal	9 Crystal Detector No.	10 Crystal Sensitivity mv/db	11 Vertical Gain mv/cm	12 Magnitude of Effect MV	13 Magnitude of Effect DB
23	16	107.5	8	Circulator with limiter tuned to 5.6 Gc attached to receiver port (Circulator-Limiter Duplexer)	5.6	0.75	Output signal from limiter	12**	5*	5	0.1	0.020
24	16	107.5	9	Front end (klystron, waveguide attenuator, coax-to-waveguide adapter, isolator) inside KIVA	5.6	~ 180	Monitor signal from front end	2	23	50	30	-1.302****

*Poor calibration sensitivity

**Crystal detector inside KIVA

***This pulse was not photographed directly due to incorrect vertical gain setting on the preamplifier. The photograph was obtained from a playback of the magnetic tape.

****This effect was an apparent decrease in the insertion loss of the components in the front end.

- The data from bursts 9, 11 and 12 (identification numbers 8, 13 and 16) indicate that the average increase in the magnitude of the insertion loss between the transmitter and antenna ports of the primary circulator due to the radiation burst is 0.05 db which was superimposed on an inherent maximum insertion loss of 0.5 db. <u>Thus, the radiation caused a 10 per cent transient increase in the insertion loss of the circulator</u>.

The data from bursts 8 and 9 (identification numbers 3, 5 and 9) were not analyzed because placement of the crystal detectors inside the KIVA degraded their performance and resulted in poor calibration and test sensitivity.

Front End Inside KIVA

- The data from bursts 13 and 14 (identification numbers 19 and 20) indicate that the average increase in the magnitude of the transmitter to antenna port insertion loss of the circulator (operating at a power level of approximately 1.75 watts) due to the radiation burst is 0.12 db superimposed on a maximum inherent insertion loss of 0.5 db. <u>Thus, the radiation caused a 24 per cent transient increase in the insertion loss of the circulator</u>.

The data from bursts 10, 11, 12 and 16 (identification numbers 12, 15, 18 and 24) are not consistent enough to justify interpretation. The magnitude of the radiation effects decreased with increased front end exposure and on the last burst an overall decrease (identification number 24) in attenuation was noted. Although it is possible to postulate that the klystron became more radiation resistant with each successive burst,

too few data have been obtained to draw a positive conclusion to this effect.

4.2.7 Results of DC Experiments

The analysis of the data from the dc experiments was performed in a different manner than that used for interpreting the microwave experiments. No calibration curves were obtained; rather, the deflection of the signal level (volts) as observed on the oscilloscope was used to calculate the amount of current which must have flowed or leaked across the open circuited component or cable at the time of the burst. The following formula (derived for the circuit shown in Figure 6) was used in perform these calculations:

$$i_3 = \frac{\Delta E \ (R_1 + R_2)}{R_1 \ R_m}$$

where

i_3 = current flowing across open circuited test component or cable, amperes

ΔE = change in signal level due to radiation burst as observed on oscilloscope, volts

R_1 = equivalent loading resistance, ohms

R_2 = resistance in parallel with test component, ohms

R_m = oscilloscope and recorder termination resistances in parallel with each other, ohms.

The results of these analyses are presented in Table 9. The susceptibility of the test specimen to a leakage current induced by the radiation is reported in terms of the effective resistance that existed between the high potential and ground planes at the time of the burst. The effective resistance was calculated by dividing the voltage applied across the component (column 6) by the leakage current (column 10). The final value of one of the resistors used in the power supply was not set until the fourth burst. Because of this, higher voltages were applied to the components during the first two bursts and a different termination resistor was used across the oscilloscope for the first three bursts.

The following qualitative conclusions were drawn from an examination of the values presented in column 11 of Table 9.

- For a positive polarity the microwave components, particularly circulators and isolators, exhibited the lowest equivalent resistance (evidenced by the low magnitude of the values in column 11 for identification numbers 14, 16, 18 and 20). Possibly, this effect is due to the very short air filled gaps between the conductor and ground planes in the components.
- The transmission lines (waveguides and coaxial cables) do not appear to have as low equivalent resistances as the components (evidenced by the relatively high values in column 11 for identification numbers 2, 4, 6, 17, 19, etc.).

Table 9. Results of Radiation Environment Tests of Various Components Subjected to High D. C. Voltages (Sheet 1 of 2)

1 Iden. No.	2 Burst No.	3 Burst Size	4 Type of Component	5 Distance from Reactor Inches	6 Applied Voltage, Volts	7 Polarity	8 Vertical Gain mv/cm	9 ΔE Volts	10 i_3 Amperes	11 Apparent Resistance Offered by Leakage Path, Ohms
1	1	100.7	Half-potted BNC double female connector	3.5	870	+	50	0.0115	13.4×10^{-6}	64.1×10^{6}
2	1	100.7	Open ended RG-58 C/U cable	3.5	880	+	50	0.0170	13.4×10^{-6}	64.8×10^{6}
3	2	107.0	Half-potted BNC double female connector	3.5	870	-	50	0.0170	19.1×10^{-6}	45.0×10^{6}
4	2	107.0	Open ended RG-58 C/U cable	3.5	880	-	50	0.0130	14.6×10^{-6}	59.4×10^{6}
5	4	108.0	Unpotted type "N" double female connector	3.5	460	-	200*	0.226	4.83×10^{-6}	90.3×10^{6}
6	4	108.0	Open circulator	3.0	440	-	200*	0.376	8.04×10^{-6}	48.5×10^{6}
7	5	109.7	Unpotted type "N" double female connector	3.5	460	+	200	0.258	5.52×10^{-6}	74.7×10^{6}
8	5	109.7	Open circulator	3.5	440	+	200	0.478	10.23×10^{-6}	37.0×10^{6}
9	6	108.0	Air filled aluminum waveguide	3.0	460	+	200	0.240	5.14×10^{-6}	84.8×10^{6}
10	6	108.0	Open limiter	3.0	440	+	200	0.296	6.33×10^{-6}	62.9×10^{6}
11	7	108.5	Unpotted BNC to type "N" connector	3.5	460	+	200	0.124	2.65×10^{-6}	169×10^{6}
12	7	108.0	Open waveguide-to-coax adapter	3.5	440	+	200	0.008	0.171×10^{-6}	251×10^{7}
13	8	109.0	Half-potted type "N" double female connector	3.5	460	+	100	0.121	2.59×10^{-6}	172×10^{6}
14	8	109.0	Open isolator in reverse direction	3.5	440	+	200*	0.826	17.68×10^{-6}	19.4×10^{6}
15	9	109.5	Half-potted type "N" double female connector	3.5	460	+	100	0.120	2.57×10^{-6}	174×10^{6}
16	9	109.5	Open isolator in forward direction	3.5	440	+	500	0.795	17.01×10^{-6}	20.3×10^{6}
17	10	114.0	Air filled brass waveguide	3.5	460	+	100	0.014	0.300×10^{-6}	153×10^{7}

Table 9. Results of Radiation Environment Tests of Various Components Subjected to High D. C. Voltages (Sheet 2 of 2)

1 Iden. No.	2 Burst No.	3 Burst Size	4 Type of Component	5 Distance from Reactor Inches	6 Applied Voltage, Volts	7 Polarity	8 Vertical Gain mv/cm	9 ΔE Volts	10 i_3 Amperes	11 Apparent Resistance Offered by Leakage Path, Ohms
18	10	114.0	Open circulator	3.5	440	+	500*	0.830	17.76×10^{-6}	19.2×10^{6}
19	11	109.5	Air filled brass waveguide	3.5	380	+	50	0.018	0.385×10^{-6}	98.3×10^{7}
20	11	109.5	Open circulator	3.5	355	+	500	0.510	10.91×10^{-6}	27.5×10^{6}
21	12	112.3	Air filled brass waveguide	3.5	235	+	50	0.0055	0.118×10^{-6}	198×10^{7}
22	12	112.3	Open circulator	3.5	225	+	200	0.344	7.3×10^{-6}	25.5×10^{6}
23	13	107.5	Open limiter	3.5	460	+	50	0.007	0.150×10^{-6}	306×10^{7}
24	13	107.5	High density Styrofoam filled brass waveguide	3.5	440	+	100	0.221	4.73×10^{-6}	81.7×10^{6}
25	14	107.2	High density Styrofoam filled brass waveguide	3.5	235	+	50	0.0055	0.118×10^{-6}	198×10^{7}
26	14	107.2	Open limiter	3.5	225	+	100	0.126	2.74×10^{-6}	77.1×10^{6}
27	15	106.0	Open isolator in forward direction	3.5	460	-	50	0.081	1.72×10^{-6}	262×10^{6}
28	15	106.0	Open ended RG-5 B/U cable	3.5	430	-	100	0.388	8.30×10^{-6}	47.7×10^{6}
29	16	107.5	Open isolator in forward direction	3.5	235	-	50	0.046	0.984×10^{-6}	234×10^{6}
30	16	107.5	Open ended RG-5 B/U cable	3.5	225	-	100	0.236	5.05×10^{-6}	39.6×10^{6}

*This pulse was not photographed directly due to incorrect vertical gain setting on the preamplifier. The photograph was obtained from a playback of the magnetic tape.

- The effective resistance appears to be dependent on the polarity (evident from a comparison of the values in column 11 for identification numbers 16 and 27) possibly implying that the radiation effect is dependent on the available electron leakage surface area.

4.3 DOSIMETRY

The burst magnitude data provided by the SPRF personnel at the time of the experiments is summarized in Table 10. The change in bulk reactor temperature during the burst is given with the total number of fissions which occurred during the burst. The latter parameter is calculated by means of the following relation[12]:

$$\text{Total number of fissions} = \frac{\Delta T\ (^\circ C)}{55} \times 10^{16}$$

The dosimetry support given by the Sandia Corporation Nuclear Measurements and Dosimetry Section consisted of the following:

(a) Four sulfur pellets per burst to measure the integrated neutron ($E_n > 3.00$ Mev) flux at each component.

(b) One each per day of plutonium, neptunium and uranium fission foils enclosed in a boron ball to measure the integral neutron fluxes where

$E_n > 0.01$ Mev for Pu threshold

$E_n > 0.7$ Mev for Np threshold

$E_n > 1.5$ Mev for U threshold

TABLE 10. SPRF BURST MAGNITUDE DATA FOR THE SECOND SPERRY MICROWAVE ELECTRONICS COMPANY EXPERIMENTAL SERIES

SPRF Burst No	SMEC Burst No.	Date	Time	ΔT, °C	Total Number of Fissions
1-41	1	1-14-63	0916	100.7	1.83×10^{16}
1-42	2	1-14-63	1052	107.0	1.95×10^{16}
1-43	3	1-14-63	1231	108.6	1.97×10^{16}
1-44	4	1-14-63	1402	108.0	1.96×10^{16}
1-54	5	1-15-63	0915	109.7	1.99×10^{16}
1-55	6	1-15-63	1044	108.0	1.96×10^{16}
1-56	7	1-15-63	1209	108.5	1.97×10^{16}
1-57	8	1-15-63	1342	109.0	1.98×10^{16}
1-58	9	1-15-63	1503	109.5	1.99×10^{16}
1-67	10	1-16-63	0838	114.0	2.07×10^{16}
1-68	11	1-16-63	1004	109.5	1.99×10^{16}
1-69	12	1-16-63	1127	112.3	2.04×10^{16}
1-70	13	1-16-63	1259	107.5	1.96×10^{16}
1-71	14	1-16-63	1432	107.2	1.95×10^{16}
1-78	15	1-17-63	0934	106.0	1.93×10^{16}
1-79	16	1-17-63	1057	107.5	1.96×10^{16}

(c) Two gold foils for each burst, one of which was cadmium covered, to measure the integrated neutron ($E_n < 0.4$ ev) flux.

(d) Three glass rods (in lithium cylinders) per burst to measure the integrated γ-ray dose in rads H_2O (In this definition 1 rad is the amount of γ radiation necessary to produce a 100 erg/gram energy absorption rate in water).

Only one set of fission foils (item b above) was used per day of testing. The $E_n > 0.01$ Mev, $E_n > 0.7$ Mev and $E_n > 1.5$ Mev integral fluxes for the other bursts obtained that day were inferred from the values measured during the burst in which the foils were present. A ratio of burst to burst integral fluxes ($E_n > 3.0$ Mev), as measured by the sulfur pellets, was used to calculate the equivalent fission foil fluxes for the other bursts obtained during the day. This procedure was suggested by SPRF personnel[13].

In order to obtain the maximum dose rates from the integral quantities reported by the Nuclear Measurements and Dosimetry Section the following procedure[14] was followed. "The reactor period associated with the burst is denoted by T. The width of the neutron pulse at one-half maximum, Tw, is given by Tw = 2.86T. For a 50-microsecond wide pulse, the period is 1.75×10^{-5} seconds or 17.5 microseconds. The reciprocal reactor period $\alpha = 1/T$ is 5.72×10^{4} sec^{-1}.

The ratio of peak fission rate to total fissions is

$$\frac{F_{max}}{F_{total}} = \frac{\alpha}{4} = 1.43 \times 10^4/\text{second for a 50-}\mu\text{sec pulse.}$$

The neutron flux above 3.0 Mev is measured by sulphur pellets which is about 14.5 per cent of the total flux above 10 Kev. The first collision tissue dose is related to the sulphur flux by $D_n = 1.66 \times 10^{-8} \phi_s$. About 80 per cent of the total neutron dose is delivered during the prompt critical burst and the remaining 20 per cent during the delayed critical portion of the burst.

Approximately 75 per cent of the total gamma dose is delivered during the prompt critical burst, and the total gamma dose is approximately 10 per cent of the total neutron dose. The peak gamma dose rate for a 50-microsecond burst then becomes $1.07 \times 10^3 D_n$, where D_n is the total neutron dose delivered during the burst." The results of these type calculations giving dose rates along with the integral doses, where available, are given in Table 11. (Which appears at the end of this section.).

The interpretations of signal level changes greater than 1 db reported in Table 11, (which appears at the end of this section) excepting the large changes observed in the front end inside the KIVA tests, were due to poor sensitivity in the calibration procedures which was generally caused by

placement of the crystal detector inside the KIVA. Changes in signal level did occur in these cases, however the magnitude of these changes was undoubtedly more of the order of tenths or hundredths of a db. Such changes would be in agreement with the results of component tests where good calibration results were obtained.

1.

1	2	3	4	5	6	7	8	9
BURST NO.	COMPONENTS EXPOSED	OPERATING FREQUENCY GC	POWER DELIVERED TO COMPONENT (MILLIWATTS)*	INTEGRATED NEUTRON FLUX $E_n > 3.0$ Mev (NEUTRONS/cm²)	INTEGRATED NEUTRON FLUX $E_n > 1.5$ Mev (NEUTRONS/cm²)	$E_n > 0.7$ Mev (NEUTRONS/cm²)	$E_n > 0.01$ Mev (NEUTRONS/cm²)	1/ SULFUR PELLET INTEGRATED NEUT $E_n > 10$ K (NEUTRONS/c
1	CIRCULATOR	5.6	160	7.26×10^{11}	2.78×10^{12}	7.31×10^{12}	9.78×10^{12}	5.01×10[illegible]
	AIR FILLED BRASS WAVEGUIDE	5.6	120	1.44×10^{12}	2.78×10^{12}	7.31×10^{12}	9.78×10^{12}	9.93×10[illegible]
	AIR FILLED ALUMINUM WAVEGUIDE	5.6	80	1.46×10^{12}	2.78×10^{12}	7.31×10^{12}	9.78×10^{12}	1.01×10[illegible]
	HALF-POTTED DOUBLE FEMALE BNC TYPE	dc	870 (+)	1.19×10^{12}	2.78×10^{12}	7.31×10^{12}	9.78×10^{12}	8.21×10[illegible]
	OPEN ENDED RG 58 C/U COAXIAL CABLE	dc	880 (+)	1.19×10^{12}	2.78×10^{12}	7.31×10^{12}	9.78×10^{12}	8.21×10[illegible]
2	CIRCULATOR	5.6	160	7.27×10^{11}	3.56×10^{12}	9.34×10^{12}	1.25×10^{13}	5.01×10[illegible]
	AIR FILLED BRASS WAVEGUIDE	5.6	120	1.52×10^{12}	3.56×10^{12}	9.34×10^{12}	1.25×10^{13}	1.05×10[illegible]
	AIR FILLED ALUMINUM WAVEGUIDE	5.6	80	1.55×10^{12}	3.56×10^{12}	9.34×10^{12}	1.25×10^{13}	1.07×10[illegible]
	HALF-POTTED DOUBLE FEMALE BNC TYPE	dc	870 (-)	1.24×10^{12}	3.56×10^{12}	9.34×10^{12}	1.25×10^{13}	8.55×10^{12}
	OPEN ENDED RG 58 C/U COAXIAL CABLE	dc	880 (-)	1.24×10^{12}	3.56×10^{12}	9.34×10^{12}	1.25×10^{13}	8.55×10^{12}
3	CIRCULATOR	5.6	160	7.72×10^{11}	2.57×10^{12}	6.75×10^{12}	9.04×10^{12}	5.32×10^{12}
	AIR FILLED BRASS WAVEGUIDE	5.6	120	1.42×10^{12}	2.57×10^{12}	6.75×10^{12}	9.04×10^{12}	9.79×10^{12}
	AIR FILLED ALUMINUM WAVEGUIDE	5.6	80	1.35×10^{12}	2.57×10^{12}	6.75×10^{12}	9.04×10^{12}	9.31×10^{12}
	HALF-POTTED DOUBLE FEMALE BNC TYPE	dc	870 (-)	1.10×10^{12}	2.57×10^{12}	6.75×10^{12}	9.04×10^{12}	7.59×10^{12}
	OPEN ENDED RG 58 C/U COAXIAL CABLE	dc	880 (-)	1.10×10^{12}	2.57×10^{12}	6.75×10^{12}	9.04×10^{12}	7.59×10^{12}
4	CIRCULATOR	5.6	60	7.56×10^{11}	2.38×10^{12}	6.26×10^{12}	8.38×10^{12}	5.21×10^{12}
	LOW DENSITY STYROFOAM FILLED BRASS WAVEGUIDE	5.6	120	1.33×10^{12}	2.38×10^{12}	6.26×10^{12}	8.38×10^{12}	9.17×10^{12}
	HIGH DENSITY STYROFOAM FILLED ALUMINUM WAVEGUIDE	5.6	80	1.19×10^{12}	2.38×10^{12}	6.26×10^{12}	8.38×10^{12}	8.21×10^{12}
	OPEN CIRCULATOR	dc	440 (-)	1.02×10^{12}	2.38×10^{12}	6.26×10^{12}	8.38×10^{12}	7.03×10^{12}
	OPEN UNPOTTED DOUBLE FEMALE "TYPE N"	dc	460 (-)	1.02×10^{12}	2.38×10^{12}	6.26×10^{12}	8.38×10^{12}	7.03×10^{12}
5	CIRCULATOR	5.6	160	7.92×10^{11}	1.73×10^{12}	3.49×10^{12}	5.76×10^{12}	5.46×10^{12}
	HIGH DENSITY STYROFOAM FILLED BRASS WAVEGUIDE	5.6	120	1.42×10^{12}	1.73×10^{12}	3.49×10^{12}	5.76×10^{12}	9.80×10^{12}
	LOW DENSITY STYROFOAM FILLED ALUMINUM WAVEGUIDE	5.6	80	9.20×10^{11}	1.73×10^{12}	3.49×10^{12}	5.76×10^{12}	6.35×10^{12}
	OPEN CIRCULATOR	dc	440 (+)	8.13×10^{11}	1.73×10^{12}	3.49×10^{12}	5.76×10^{12}	5.61×10^{12}
	OPEN UNPOTTED DOUBLE FEMALE "TYPE N"	dc	460 (+)	8.13×10^{11}	1.73×10^{12}	3.49×10^{12}	5.76×10^{12}	5.61×10^{12}
6	CIRCULATOR	5.6	160	7.65×10^{11}	2.02×10^{12}	4.07×10^{12}	6.72×10^{12}	5.30×10^{12}
	TWO WAVEGUIDE-TO-COAX ADAPTERS BUTTED TOGETHER	5.6	120	1.58×10^{12}	2.02×10^{12}	4.07×10^{12}	6.72×10^{12}	1.09×10^{13}
	ISOLATOR OPERATING IN FORWARD DIRECTION	5.6	80	9.48×10^{11}	2.02×10^{12}	4.07×10^{12}	6.72×10^{12}	6.54×10^{12}
	AIR FILLED ALUMINUM WAVEGUIDE	dc	460 (+)	9.48×10^{11}	2.02×10^{12}	4.07×10^{12}	6.72×10^{12}	6.54×10^{12}
	OPEN LIMITER	dc	440 (+)	9.48×10^{11}	2.02×10^{12}	4.07×10^{12}	6.72×10^{12}	6.54×10^{12}
7	CIRCULATOR	5.6	160	6.99×10^{11}	1.50×10^{12}	3.02×10^{12}	4.99×10^{12}	4.82×10^{12}
	LIMITER	5.6	120	6.94×10^{11}	1.50×10^{12}	3.02×10^{12}	4.99×10^{12}	4.79×10^{12}
	ISOLATOR OPERATING IN REVERSE DIRECTION	5.6	80	1.00×10^{12}	1.50×10^{12}	3.02×10^{12}	4.99×10^{12}	6.90×10^{12}
	OPEN UNPOTTED BNC TO "TYPE N" CONNECTOR	dc	460 (+)	7.04×10^{11}	[illegible]	3.02×10^{12}	4.99×10^{12}	4.86×10^{12}
	OPEN WAVEGUIDE-TO-COAX ADAPTER	dc	440 (+)	[illegible]	[illegible]	3.02×10^{12}	4.99×10^{12}	[illegible]
8	TWO CIRCULATORS IN TANDEM	5.6	160	[illegible]	[illegible]	[illegible]	[illegible]	[illegible]
	CIRCULATOR-LIMITER DUPLEXER	5.6	120	7.03×10^{11}	1.52×10^{12}	3.05×10^{12}	5.05×10^{12}	4.85×10^{12}
	ISOLATOR OPERATING IN REVERSE DIRECTION	5.6	80	9.91×10^{11}	1.52×10^{12}	3.05×10^{12}	5.05×10^{12}	6.83×10^{12}
	OPEN ISOLATOR IN REVERSE DIRECTION	dc	440 (+)	7.12×10^{11}	1.52×10^{12}	3.05×10^{12}	5.05×10^{12}	4.91×10^{12}
	HALF-POTTED DOUBLE FEMALE, "TYPE N"	dc	460 (+)	7.12×10^{11}	1.52×10^{12}	3.05×10^{12}	5.05×10^{12}	4.91×10^{12}

TABLE 11. NEUTR
AND D

	8	9	10	11	12	13	14	15	16	
EUTRON FLUX Mev cm2)	E_n > 0.01 Mev (NEUTRONS/cm^2)	$\phi_{SULFUR\ PELLET}$ INTEGRATED NEUTRON FLUX E_n > 10 Kev (NEUTRONS/cm^2)	INTEGRATED NEUTRON FLUX E_n < 0.4 ev (NEUTRONS/cm^2)	$D_n = 1.66 \times 10^{-9} \phi_{SULFUR\ PELLET}$ NEUTRON TISSUE DOSE, RAD	PULSE WIDTH AT HALF-MAX. DETERMINED FOM SPRF PHOTOGRAPH, SEC.	$\tau = \frac{\text{PULSE WIDTH}}{2.86}$ REACTOR PERIOD, SEC.	$1/4\tau$ F_{MAX}/F_{TOTAL}	F_M/F_T (ϕE_n > 10 Kev) PEAK INCIDENT NEUTRON FLUX (NEUTRON/cm^2 SEC.)	INTEGRATED GAMMA DOSE, RADS (H_2O)	1.07 x PEAK I GAMMA RADS
12	9.78×10^{12}	5.01×10^{12}	NOT AVAILABLE	1.21×10^{4}	55×10^{-6}	19.2×10^{-6}	1.30×10^{4}	6.51×10^{16}	1.70×10^{3}	1.29
12	9.78×10^{12}	9.93×10^{12}	NOT AVAILABLE	2.39×10^{4}	55×10^{-6}	19.2×10^{-6}	1.30×10^{4}	1.29×10^{17}	3.38×10^{3}	2.56
12	9.78×10^{12}	1.01×10^{13}	NOT AVAILABLE	2.42×10^{4}	55×10^{-6}	19.2×10^{-6}	1.30×10^{4}	1.31×10^{17}	[illegible]	2.59
12	9.78×10^{12}	8.21×10^{12}	NOT AVAILABLE	1.97×10^{4}	55×10^{-6}	19.2×10^{-6}	[illegible]	[illegible]	[illegible]	2.11
12	9.78×10^{12}	8.21×10^{12}	NOT AVAILABLE	1.97×10^{4}	55×10^{-6}	19.2×10^{-6}	[illegible]	[illegible]	[illegible]	2.11
12	1.25×10^{13}	5.01×10^{12}	1.63×10^{10}	1.21×10^{4}	54×10^{-6}	18.9×10^{-6}	[illegible]	[illegible]	[illegible]	1.29
12	1.25×10^{13}	1.05×10^{13}	1.63×10^{10}	2.57×10^{4}	54×10^{-6}	18.9×10^{-6}	[illegible]	[illegible]	[illegible]	[illegible]
12	1.25×10^{13}	1.07×10^{13}	1.63×10^{10}	2.52×10^{4}	54×10^{-6}	18.9×10^{-6}	[illegible]	[illegible]	[illegible]	[illegible]
12	1.25×10^{13}	8.55×10^{12}	1.63×10^{10}	2.06×10^{4}	54×10^{-6}	18.9×10^{-6}	[illegible]		[illegible]	[illegible]
12	1.25×10^{13}	8.55×10^{12}	1.63×10^{10}	[illegible]	54×10^{-6}	[illegible]	[illegible]		[illegible]	[illegible]
12	9.04×10^{12}	5.32×10^{12}	1.67×10^{10}	1.28×10^{4}	57×10^{-6}	19.9×10^{-6}	[illegible]		[illegible]	[illegible]
12	9.04×10^{12}	9.79×10^{12}	1.67×10^{10}	2.35×10^{4}	57×10^{-6}	19.9×10^{-6}	[illegible]			[illegible]
12	9.04×10^{12}	9.31×10^{12}	1.67×10^{10}	[illegible]	57×10^{-6}	19.9×10^{-6}	[illegible]		[illegible]	[illegible]
12	9.04×10^{12}	7.59×10^{12}	1.67×10^{10}	1.83×10^{4}	57×10^{-6}	19.9×10	[illegible]	[illegible]	[illegible]	[illegible]
12	9.04×10^{12}	7.59×10^{12}	1.67×10^{10}	1.83×10^{4}	57×10^{-6}	19.9×10^{-6}	[illegible]	[illegible]	[illegible]	[illegible]
12	8.38×10^{12}	5.21×10^{12}	1.72×10^{10}	[illegible]	57×10^{-6}	[illegible]	[illegible]	[illegible]	[illegible]	[illegible]
12	8.38×10^{12}	9.17×10^{12}	1.72×10^{10}	2.21×10^{4}	57×10^{-6}	19.9×10^{-6}	[illegible]	[illegible]	[illegible]	[illegible]
12	8.38×10^{12}	8.21×10^{12}	1.72×10^{10}	1.98×10^{4}	57×10^{-6}	[illegible]	[illegible]	[illegible]	[illegible]	[illegible]
12	8.38×10^{12}	7.03×10^{12}	1.72×10^{10}	[illegible]	57×10^{-6}	[illegible]	[illegible]	[illegible]	[illegible]	1.81
12	8.38×10^{12}	7.03×10^{12}	1.72×10^{10}	[illegible]	57×10^{-6}	19.9×10^{-6}	[illegible]	[illegible]	[illegible]	1.81
12	5.76×10^{12}	5.46×10^{12}	1.67×10^{10}	1.32×10^{4}	50×10^{-6}	17.5×10^{-6}	1.43×10^{4}	[illegible]	[illegible]	1.41
12	5.76×10^{12}	9.80×10^{12}	1.67×10^{10}	2.36×10^{4}	50×10^{-6}	[illegible]	1.43×10^{4}	[illegible]	[illegible]	[illegible]
12	5.76×10^{12}	6.35×10^{12}	1.67×10^{10}	[illegible]	50×10^{-6}	17.5×10^{-6}	1.43×10^{4}	[illegible]	[illegible]	1.64
12	5.76×10^{12}	5.61×10^{12}	1.67×10^{10}	1.35×10^{4}	50×10^{-6}	17.5×10^{-6}	1.43×10^{4}	8.02×10^{16}	2.24×10^{3}	1.44
12	5.76×10^{12}	5.61×10^{12}	1.67×10^{10}	1.35×10^{4}	[illegible]	17.5×10^{-6}	1.43×10^{4}	[illegible]	[illegible]	1.44
2	6.72×10^{12}	5.30×10^{12}	1.67×10^{10}	[illegible]	50×10^{-6}	17.5×10^{-6}	1.43×10^{4}	[illegible]	[illegible]	1.37
2	6.72×10^{12}	1.09×10^{13}	1.67×10^{10}	2.62×10^{4}	50×10^{-6}	17.5×10^{-6}	1.43×10^{4}	[illegible]	[illegible]	2.80
2	6.72×10^{12}	6.54×10^{12}	1.67×10^{10}	1.57×10^{9}	50×10^{-6}	17.5×10^{-6}	1.43×10^{4}	9.35×10^{16}	1.74×10^{3}	1.68
2	6.72×10^{12}	6.54×10^{12}	1.67×10^{10}	1.57×10^{4}	50×10^{-6}	17.5×10^{-6}	1.43×10^{4}	9.35×10^{16}	[illegible]	1.68
2	6.72×10^{12}	6.54×10^{12}	1.67×10^{10}	1.57×10^{4}	50×10^{-6}	17.5×10^{-6}	1.43×10^{4}	9.35×10^{16}	1.81×10^{3}	1.68
2	4.99×10^{12}	4.82×10^{12}	1.49×10^{10}	1.16×10^{4}	52×10^{-6}	[illegible]	1.37×10^{4}	6.60×10^{16}	[illegible]	[illegible]
2	4.99×10^{12}	4.79×10^{12}	1.49×10^{10}	1.15×10^{4}	52×10^{-6}	18.2×10^{-6}	1.37×10^{4}	6.56×10^{16}	1.90×10^{3}	1.23
2	4.99×10^{12}	6.90×10^{12}	1.49×10^{10}	1.66×10^{4}	52×10^{-6}	18.2×10^{-6}	1.37×10^{4}	9.45×10^{16}	2.31×10^{3}	1.78
2	4.99×10^{12}	4.86×10^{12}	1.49×10^{10}	[illegible]	[illegible]	[illegible]	1.37×10^{4}	[illegible]	1.98×10^{3}	1.25
2	4.99×10^{12}	[illegible]	[illegible]	[illegible]	[illegible]	[illegible]	[illegible]	[illegible]	[illegible]	1.25
2	5.05×10^{12}	[illegible]	[illegible]	[illegible]	[illegible]	[illegible]	[illegible]	[illegible]	[illegible]	[illegible]
2	5.05×10^{12}	4.85×10^{12}	1.69×10^{10}	1.17×10^{4}	[illegible]	17.5×10^{-6}	1.43×10^{4}	6.94×10^{16}	2.72×10^{3}	[illegible]
2	5.05×10^{12}	6.83×10^{12}	1.69×10^{10}	1.65×10^{4}	50×10^{-6}	17.5×10^{-6}	1.43×10^{4}	9.77×10^{16}	2.55×10^{3}	[illegible]
2	5.05×10^{12}	4.91×10^{12}	1.69×10^{10}	1.18×10^{4}	50×10^{-6}	17.5×10^{-6}	1.43×10^{4}	[illegible]	2.32×10^{3}	[illegible]
2	5.05×10^{12}	4.91×10^{12}	1.69×10^{10}	1.18×10^{4}	50×10^{-6}	17.5×10^{-6}	1.43×10^{4}	[illegible]	2.32×10^{3}	[illegible]

TABLE 11. NEUTRON AND γ - RAY DOSIMETRY PROVIDING INTEGRAL DOSE AND DOSE RATE EXPOSURES TO THE MICROWAVE COMPONENTS

(SHEET 1)

11	12	13	14	15	16	17	18
=1.66x10^-8 ∫ SULFUR PELLET NEUTRON TISSUE DOSE, RAD	PULSE WIDTH AT HALF-MAX. DETERMINED FOM SPRF PHOTOGRAPH, SEC.	T = PULSE WIDTH / 2.86 REACTOR PERIOD, SEC.	1.4T F_{MAX} / F_{TOTAL}	[illegible] PEAK INCIDENT NEUTRON FLUX (NEUTRON/cm^2-SEC.)	INTEGRATED GAMMA DOSE, RADS (H_2O)	1.07×10^3 D_n PEAK INCIDENT GAMMA DOSE RADS/SEC.	RADIATION EFFECT ON COMPONENT
1.21×10^4	55×10^{-6}	19.2×10^{-6}	1.30×10^4	6.51×10^{16}	1.70×10^3	1.29×10^7	0.03 DB INCREASE IN INSERTION LOSS
2.39×10^4	55×10^{-6}	19.2×10^{-6}	1.30×10^4	1.29×10^{17}	3.38×10^3	2.56×10^7	0.10 DB INCREASE IN ISOLATION 0.16 DB INCREASE IN ATTENUATION
2.42×10^4	55×10^{-6}	19.2×10^{-6}	1.30×10^4	1.31×10^{17}	2.88×10^3	2.59×10^7	NONE OBSERVED
1.97×10^4	55×10^{-6}	19.2×10^{-6}	1.30×10^4	1.97×10^{17}	2.60×10^3	2.11×10^7	64.1×10^6 Ω APPARENT RESISTANCE ACROSS COMPONENT
1.97×10^4	55×10^{-6}	19.2×10^{-6}	1.30×10^4	1.07×10^{17}	2.60×10^3	2.11×10^7	64.8×10^6 Ω APPARENT RESISTANCE ACROSS COMPONENT
1.21×10^4	54×10^{-6}	18.9×10^{-6}	1.32×10^4	6.61×10^{16}	1.97×10^3	1.29×10^7	NONE OBSERVED
2.57×10^4	54×10^{-6}	18.9×10^{-6}	1.32×10^4	1.39×10^{17}	3.72×10^3	2.70×10^7	0.335 DB INCREASE IN ATTENUATION
2.52×10^4	54×10^{-6}	18.9×10^{-6}	1.32×10^4	1.31×10^{17}	2.81×10^3	2.75×10^7	0.224 DB INCREASE IN ATTENUATION
[illegible].06 x 10^4	54×10^{-6}	18.9×10^{-6}	1.32×10^4	1.13×10^{17}	2.89×10^3	2.20×10^7	4[?].0 x 10^6 Ω APPARENT RESISTANCE ACROSS COMPONENT
[illegible] x 10^4	54×10^{-6}	18.9×10^{-6}	1.32×10^4	1.13×10^{17}	2.89×10^3	2.20×10^7	59.4×10^6 APPARENT RESISTANCE ACROSS COMPONENT
1.28×10^4	57×10^{-6}	19.9×10^{-6}	1.25×10^4	6.65×10^{16}	1.54×10^3	1.37×10^7	0.052 DB INCREASE IN INSERTION LOSS
2.35×10^4	57×10^{-6}	19.9×10^{-6}	1.25×10^4	1.2[?] x 10^{17}	3.1[?] x 10^3	2.51×10^7	0.054 DB INCREASE IN ISOLATION 0.369 DB INCREASE IN ATTENUATION
2.25×10^4	57×10^{-6}	19.9×10^{-6}	1.25×10^4	1.16×10^{17}	2.88×10^3	2.41×10^7	0.312 DB INCREASE IN ATTENUATION
1.83×10^4	57×10^{-6}	19.9×10^{-6}	1.25×10^4	[?].49 x 10^{16}	2.58×10^3	1.96×10^7	NONE OBSERVED
1.83×10^4	57×10^{-6}	19.9×10^{-6}	1.25×10^4	[?].49 x 10^{16}	2.58×10^3	1.96×10^7	NONE OBSERVED
1.26×10^4	57×10^{-6}	19.9×10^{-6}	1.25×10^4	6.51×10^{16}	1.6[?] x 10^3	1.36×10^7	0.06 DB INCREASE IN INSERTION LOSS
2.21×10^4	57×10^{-6}	19.9×10^{-6}	1.25×10^4	1.1[?] x 10^{17}	[illegible]	2.36×10^7	0.12 DB INCREASE IN ISOLATION 0.922 DB INCREASE IN ATTENUATION
[?].98 x 10^4	57×10^{-6}	19.9×10^{-6}	1.25×10^4	1.13 x [illegible]	[?].15 x 10^3	2.12×10^7	0.091 DB INCREASE IN ATTENUATION
[?].69 x 10^4	57×10^{-6}	19.9×10^{-6}	1.25×10^4	8.79 x [illegible]	[illegible]	1.81×10^7	48.5×10^6 APPARENT RESISTANCE ACROSS COMPONENT
[?].69 x 10^4	57×10^{-6}	19.9×10^{-6}	1.25 x [illegible]	8.79 x [illegible]	2.23×10^3	1.81×10^7	90.3×10^6 Ω APPARENT RESISTANCE ACROSS COMPONENT
.32 x 10^4	50×10^{-6}	17.5×10^{-6}	1.43×10^4	[?].81 x 10^{16}	[illegible]	1.41×10^7	0.043 DB INCREASE IN INSERTION LOSS
.36 x 10^4	50×10^{-6}	17.5×10^{-6}	1.43×10^4	1.40×10^{17}	3.12×10^3	2.53×10^7	0.095 DB INCREASE IN ISOLATION 0.103 DB INCREASE IN ATTENUATION
.53 x 10^4	50×10^{-6}	17.5×10^{-6}	1.43×10^4	9.08×10^{16}	2.15×10^3	1.61×10^7	0.012 DB CHANCE IN VSWR SIGNAL 0.703 DB INCREASE IN ATTENUATION
.35 x 10^4	50×10^{-6}	17.5×10^{-6}	1.43×10^4	8.02×10^{16}	2.24×10^3	1.44×10^7	37.0×10^6 APPARENT RESISTANCE ACROSS COMPONENT
.35 x 10^4	50×10^{-6}	17.5×10^{-6}	1.43×10^4	[illegible] x 10^{16}	2.24×10^3	1.44×10^7	74.7×10^6 APPARENT RESISTANCE ACROSS COMPONENT
.26 x 10^4	50×10^{-6}	17.5×10^{-6}	1.43×10^4	7.56×10^{16}	1.60 x [illegible]	1.37×10^7	0.049 DB INCREASE IN INSERTION LOSS
.62 x 10^4	50×10^{-6}	17.5×10^{-6}	1.43×10^4	1.56 x [illegible]	3.21 x [illegible]	2.80×10^7	0.100 DB INCREASE IN ISOLATION 0.196 DB INCREASE IN ATTENUATION
.57 x 10^4	50×10^{-6}	17.5×10^{-6}	1.43×10^4	9.[?] x 10^{16}	1.74×10^3	1.68×10^7	0.035 DB CHANGE IN VSWR SIGNAL 0.097 DB INCREASE IN INSERTION LOSS
57 x 10^4	50×10^{-6}	17.5×10^{-6}	1.43×10^4	9.35×10^{16}	1.81×10^3	1.68×10^7	8[?].8 x 10^6 APPARENT RESISTANCE ACROSS COMPONENT
57 x 10^4	50×10^{-6}	17.5×10^{-6}	1.43×10^4	9.[?] x 10^{16}	[?].81 x 10^3	1.68×10^7	62.9×10^6 APPARENT RESISTANCE ACROSS COMPONENT
16 x 10^4	52×10^{-6}	18.2×10^{-6}	1.37×10^4	6.63×10^{16}	1.54 x [illegible]	1.24×10^7	0.047 DB INCREASE IN INSERTION LOSS
15 x 10^4	52×10^{-6}	18.2×10^{-6}	1.37×10^4	6.56×10^{16}	1.90×10^3	1.23×10^7	0.075 DB INCREASE IN ISOLATION 0.104 DB INCREASE IN INSERTION LOSS
66 x 10^4	52×10^{-6}	18.2×10^{-6}	1.37×10^4	9.45×10^{16}	2.31×10^3	1.78×10^7	0.019 DB CHANGE IN VSWR SIGNAL 0.062 DB INCREASE IN ISOLATION
17 x 10^4	[illegible]	18.2×10^{-6}	1.37×10^4	6.66×10^{16}	1.98×10^3	1.25×10^7	169×10^6 APPARENT RESISTANCE ACROSS COMPONENT
[illegible] 10^4	[illegible]	[illegible]	1.37×10^4	6.[?] x 10^{16}	1.98×10^3	1.25×10^7	251 x 10^7 APPARENT RESISTANCE
[illegible] 10^4	[illegible]	[illegible]	[illegible]	[illegible]	1.67 x 10^3	[illegible] x 10^7	0.446 DB INCREASE IN ISOLATION OF PRIMARY CIRCULATOR
17 x 10^4	50×10^{-6}	17.5×10^{-6}	1.43×10^4	6.94×10^{16}	2.72×10^3	1.26×10^7	0.850 DB CHANGE IN VSWR SIGNAL 0.050 DB INCREASE IN INSERTION LOSS OF DEVICE 0.030 DB CHANGE IN VSWR SIGNAL ~ 2.75 DB INCREASE IN INSERION LOSS OF CIRCULATOR
[?]5 x 10^4	50×10^{-6}	17.5×10^{-6}	1.43×10^4	9.77×10^{16}	2.55×10^3	1.77×10^7	1.49 DB INCREASE IN ISOLATION
8 x 10^4	50×10^{-6}	17.5×10^{-6}	1.43×10^4	7.02×10^{16}	2.32×10^3	1.26×10^7	19.4×10^6 APPARENT RESISTANCE ACROSS COMPONENT
8 x 10^4	50×10^{-6}	17.5×10^{-6}	1.43×10^4	7.02×10^{16}	2.32×10^3	1.26×10^7	172×10^6 APPARENT RESISTANCE ACROSS COMPONENT

* In dc experiments voltage across components is indicated in volts and polarities are shown.

FOR OFFICIAL USE ONLY

3

1	2	3	4	5	6	7	8	9	10
BURST NO.	COMPONENTS EXPOSED	OPERATING FREQUENCY (Gc)	POWER DELIVERED TO COMPONENT (MILLIWATTS)	INTEGRATED NEUTRON FLUX E_n > 3.0 Mev (NEUTRONS/cm^2)	INTEGRATED NEUTRON FLUX E_n > 1.5 Mev (NEUTRONS/cm^2)	INTEGRATED NEUTRON FLUX E_n > 0.7 Mev (NEUTRONS/cm^2)	INTEGRATED NEUTRON FLUX E_n > 0.01 Mev (NEUTRONS/cm^2)	SULFUR PELLET/0.145 INTEGRATED NEUTRON FLUX E_n > 10 Kev (NEUTRONS/cm^2)	INTEGRATED NEUTRON FLUX E_n > 0.4 ev (NEUTRONS/cm^2)
9	TWO CIRCULATORS IN TANDEM	[illegible]	100	9.28×10^{11}	2.02×10^{12}	4.08×10^{12}	6.73×10^{12}	6.40×10^{12}	1.83×10^{10}
	CIRCULATOR-LIMITER DUPLEXER	5.6	100	6.70×10^{11}	2.02×10^{12}	4.08×10^{12}	6.73×10^{12}	4.62×10^{12}	1.83×10^{10}
	ISOLATOR OPERATING IN REVERSE DIRECTION	5.6	80	1.01×10^{12}	2.02×10^{12}	4.08×10^{12}	6.73×10^{12}	6.97×10^{12}	1.83×10^{10}
	GEN ISOLATOR IN FORWARD DIRECTION	16	440 (+)	9.50×10^{11}	2.02×10^{12}	4.08×10^{12}	6.73×10^{12}	6.55×10^{12}	1.83×10^{10}
	HALF-POTTED DOUBLE FEMALE TYPE N	16	440 (+)	9.50×10^{11}	2.02×10^{12}	4.08×10^{12}	6.73×10^{12}	6.55×10^{12}	1.83×10^{10}
10	TWO CIRCULATORS IN TANDEM	[illegible]	100	7.90×10^{11}	[illegible]	4.75×10^{12}	4.45×10^{12}	5.45×10^{12}	1.18×10^{10}
	CIRCULATOR	[illegible]	100	1.11×10^{12}	[illegible]	[illegible]	$4.4[illegible] \times 10^{12}$	[illegible]	1.18×10^{10}
	KLYSTRON, VARIABLE ATTENUATOR, ADAPTER, LIMITER	[illegible]	KLYSTRON OPERATING AT 2.0 W	NOT AVAILABLE	NOT AVAILABLE	NOT AVAILABLE	NOT AVAILABLE	NOT AVAILABLE	NOT AVAILABLE
	GEN ISOLATOR	16	440 (+)	1.12×10^{12}	[illegible]	[illegible]	$4.4[illegible]$	[illegible]	1.18×10^{10}
	[illegible] WAVEGUIDE	[illegible]	440 (+)	$1.1[illegible] \times 10^{12}$	1.34×10^{12}	$4.7[illegible] \times 10^{12}$	4.45×10^{12}	7.72×10^{12}	1.18×10^{10}
[illegible]	[illegible] IN TANDEM	[illegible]	100	$7.2[illegible] \times 10^{11}$	[illegible]	[illegible]	[illegible]	[illegible]	1.42×10^{10}
	[illegible]	[illegible]	KLYSTRON OPERATING AT 2.0 W	[illegible] NOT AVAILABLE	NOT AVAILABLE NOT AVAILABLE	NOT AVAILABLE NOT AVAILABLE	NOT AVAILABLE NOT AVAILABLE	$[illegible] \times 10^{11}$ NOT AVAILABLE	NOT AVAILABLE NOT AVAILABLE
	[illegible]	[illegible]	[illegible] (+)	9.74×10^{11}	[illegible]	[illegible]	[illegible]	$6.7[illegible] \times 10^{12}$	1.42×10^{10}
	[illegible]	[illegible]	[illegible] (+)	9.74×10^{11}	[illegible]	[illegible]	[illegible]	[illegible]	1.42×10^{10}
	[illegible]	[illegible]	[illegible]	[illegible]	[illegible]	[illegible]	4.81×10^{12}	[illegible]	[illegible]
	[illegible]	[illegible]	KLYSTRON OPERATING AT 2.0 W	1.04×10^{12} NOT AVAILABLE	NOT AVAILABLE	NOT AVAILABLE	NOT AVAILABLE	[illegible]	NOT AVAILABLE
	[illegible]	[illegible]	[illegible] (+)	[illegible]	[illegible]	[illegible]	[illegible]	[illegible]	[illegible]
	[illegible] WAVEGUIDE	[illegible]	[illegible] (+)	[illegible]	[illegible]	[illegible]	[illegible]	8.34×10^{12}	1.57×10^{10}
[illegible]	CIRCULATOR	[illegible]	100	[illegible]	[illegible]	[illegible]	4.05×10^{12}	4.94×10^{12}	[illegible]
	CIRCULATOR	[illegible]	100	[illegible]	NOT AVAILABLE	NOT AVAILABLE	NOT AVAILABLE	[illegible]	NOT AVAILABLE
	KLYSTRON, VARIABLE ATTENUATOR, ADAPTER, [illegible] CIRCULATOR AND [illegible]	[illegible]	KLYSTRON OPERATING AT 2.0 W	NOT AVAILABLE	NOT AVAILABLE	NOT AVAILABLE	NOT AVAILABLE	NOT AVAILABLE	NOT AVAILABLE
	[illegible]	[illegible]	440 (+)	[illegible]	[illegible]	[illegible]	[illegible]	[illegible]	[illegible]
	[illegible] WAVEGUIDE	[illegible]	440 (+)	[illegible]	[illegible]	[illegible]	[illegible]	[illegible]	1.41×10^{10}
[illegible]	CIRCULATOR	[illegible]	100	[illegible]	1.40×10^{12}	4.08×10^{12}	[illegible]	[illegible]	1.47×10^{10}
	[illegible]	[illegible]	100	[illegible]	NOT AVAILABLE	NOT AVAILABLE	NOT AVAILABLE	[illegible]	NOT AVAILABLE
	KLYSTRON, VARIABLE ATTENUATOR, ADAPTER, ISOLATOR FRONT END LIMITER	[illegible]	KLYSTRON OPERATING AT 2.0 W	NOT AVAILABLE	NOT AVAILABLE	NOT AVAILABLE	NOT AVAILABLE	NOT AVAILABLE	NOT AVAILABLE
	GEN LIMITER	[illegible]	[illegible] (+)	[illegible]	1.40×10^{12}	[illegible]	[illegible]	6.41×10^{12}	1.47×10^{10}
	[illegible] STYROFOAM [illegible] WAVEGUIDE	[illegible]	[illegible] (+)	[illegible]	1.40×10^{12}	[illegible]	[illegible]	[illegible]	1.47×10^{10}
	CIRCULATOR	[illegible]	100	8.09×10^{11}	[illegible]	2.89×10^{12}	[illegible]	[illegible]	[illegible]
	CIRCULATOR-LIMITER DUPLEXER	[illegible]	100	7.35×10^{11}	1.02×10^{12}	2.89×10^{12}	[illegible]	[illegible]	[illegible]
	KLYSTRON, VARIABLE ATTENUATOR, ADAPTER, TEE, ISOLATOR FRONT END	[illegible]	KLYSTRON OPERATING AT 2.0 W	NOT AVAILABLE	NOT AVAILABLE	NOT AVAILABLE	NOT AVAILABLE	NOT AVAILABLE	NOT AVAILABLE
	LIMITER	[illegible]	800	5.33×10^{11}	1.02×10^{12}	2.89×10^{12}	[illegible]	3.68×10^{12}	1.22×10^{10}
	GEN ISOLATOR	[illegible]	4[illegible] (+)	8.09×10^{11}	1.02×10^{12}	2.89×10^{12}	[illegible]	$5.[illegible] \times 10^{12}$	1.22×10^{10}
	[illegible]	[illegible]	4[illegible] (+)	[illegible]	1.02×10^{12}	2.89×10^{12}	[illegible]	5.58×10^{12}	[illegible]
	CIRCULATOR	[illegible]	100	3.10×10^{11}	1.02×10^{12}	2.89×10^{12}	[illegible]	[illegible]	1.21×10^{10}
	CIRCULATOR-LIMITER DUPLEXER	5.6	100	[illegible]	1.02×10^{12}	2.89×10^{12}	3.32×10^{12}	4.78×10^{12}	[illegible]
	KLYSTRON, VARIABLE ATTENUATOR, ADAPTER, TEE, ISOLATOR FRONT END	5.6	KLYSTRON OPERATING AT 2.0 W	NOT AVAILABLE	NOT AVAILABLE	NOT AVAILABLE	NOT AVAILABLE	NOT AVA[illegible]	[illegible]
	LIMITER	5.6	800	5.66×10^{11}	1.02×10^{12}	2.89×10^{12}	3.32×10^{12}	$3.90 \times$ [illegible]	[illegible]
	GEN ISOLATOR	16	225 (+)	8.10×10^{11}	1.02×10^{12}	2.89×10^{12}	3.32×10^{12}	$5.59 \times$ [illegible]	[illegible]
	OPEN ENDED RG [illegible] COAXIAL CABLE	16	225 (+)	8.10×10^{11}	1.02×10^{12}	2.89×10^{12}	3.32×10^{12}	$5.59 \times$ [illegible]	[illegible]

TABL

7	8	9	10	11	12	13	14	15	16
INTEGRATED NEUTRON FLUX E_n > 0.7 Mev (NEUTRONS/cm^2)	E_n 0.01 Mev (NEUTRONS/cm^2)	$\int\phi_{SULFUR\ PELLET}dt/0.145$ INTEGRATED NEUTRON FLUX E_n > 10 Kev (NEUTRONS/cm^2)	INTEGRATED NEUTRON FLUX E_n 0.4 ev (NEUTRONS/cm^2)	D_n $1.66\times10^{-8}\int\phi_{SULFUR\ PELLET}dt$ NEUTRON TISSUE DOSE, RAD	PULSE WIDTH AT HALF-MAX. DETERMINED FROM CPRF PHOTOGRAPH, SEC.	τ $\frac{\text{PULSE WIDTH}}{2.86}$ REACTOR PERIOD, SEC	1/4T F_{MAX}/F_{TOTAL}	$F_m/F_t\int\phi E_n$ > 10 kevdt PEAK INCIDENT NEUTRON FLUX (NEUTRON/cm^2 SEC.)	INTEGRA GAMMA DC RADS (H
4.08×10^{12}	6.73×10^{12}	6.40×10^{12}	1.83×10^{10}	1.54×10^{4}	50×10^{-6}	17.5×10^{-6}	1.43×10^{4}	9.15×10^{16}	2.63 x 1
4.08×10^{12}	6.73×10^{12}	4.62×10^{12}	1.83×10^{10}	1.11×10^{4}	50×10^{-6}	17.5×10^{-6}	1.43×10^{4}	6.61×10^{16}	2.79 x 1
4.08×10^{12}	6.73×10^{12}	6.97×10^{12}	1.83×10^{10}	1.68×10^{4}	50×10^{-6}	17.5×10^{-6}	1.43×10^{4}	9.97×10^{16}	3.12 x 1
4.08×10^{12}	6.73×10^{12}	6.55×10^{12}	1.83×10^{10}	1.58×10^{4}	50×10^{-6}	17.5×10^{-6}	1.43×10^{4}	9.37×10^{16}	2.72 x 1
4.08×10^{12}	6.73×10^{12}	6.55×10^{12}	1.83×10^{10}	1.58×10^{4}	50×10^{-6}	17.5×10^{-6}	1.43×10^{4}	9.37×10^{16}	2.72 x 1
3.75×10^{12}	4.45×10^{12}	5.45×10^{12}	1.18×10^{10}	1.31×10^{4}	50×10^{-6}	17.5×10^{-6}	1.43×10^{4}	7.79×10^{16}	1.72 x 1
3.75×10^{12}	4.45×10^{12}	[illegible] $\times 10^{12}$	1.18×10^{10}	1.84×10^{4}	50×10^{-6}	17.5×10^{-6}	1.43×10^{4}	1.10×10^{17}	2.24 x 1
NOT AVAILABLE	NOT AVAILABLE	NOT AVAILABLE	NOT AVAILABLE	NOT AVAILABLE	50×10^{-6}	17.5×10^{-6}	1.43×10^{4}	NOT AVAILABLE	NOT AVAI
3.75×10^{12}	4.45×10^{12}	7.72×10^{12}	1.18×10^{10}	1.86×10^{4}	50×10^{-6}	17.5×10^{-6}	1.43×10^{4}	1.10×10^{17}	2.34 x 1
3.75×10^{12}	4.45×10^{12}	7.72×10^{12}	1.18×10^{10}	1.86×10^{4}	50×10^{-6}	17.5×10^{-6}	1.43×10^{4}	1.10×10^{17}	2.34 x 1
3.26×10^{12}	3.87×10^{12}	5.00×10^{12}	1.42×10^{10}	1.20×10^{4}	50×10^{-6}	17.5×10^{-6}	1.43×10^{4}	7.15×10^{16}	1.64 x 1
NOT AVAILABLE	NOT AVAILABLE	4.53×10^{11}	NOT AVAILABLE	$8.50 \times 10^{[illegible]}$	50×10^{-6}	17.5×10^{-6}	1.43×10^{4}	5.05×10^{15}	1.27 x 1
NOT AVAILABLE	NOT AVAILABLE	NOT AVAILABLE	NOT AVAILABLE	NOT AVAILABLE	50×10^{-6}	17.5×10^{-6}	1.43×10^{4}	NOT AVAILABLE	NOT AVAIL
3.26×10^{12}	3.87×10^{12}	6.72×10^{12}	1.42×10^{10}	1.62×10^{4}	50×10^{-6}	17.5×10^{-6}	1.43×10^{4}	9.61×10^{16}	2.31 x 1
3.26×10^{12}	3.87×10^{12}	6.72×10^{12}	1.42×10^{10}	1.62×10^{4}	50×10^{-6}	17.5×10^{-6}	1.43×10^{4}	9.61×10^{16}	2.31 x 1
4.05×10^{12}	4.81×10^{12}	[illegible] $\times 10^{12}$	1.57×10^{1}	$1.2[illegible] \times 10^{4}$	50×10^{-6}	17.5×10^{-6}	1.43×10^{4}	7.28×10^{16}	1.39 x 1
NOT AVAILABLE	NOT AVAILABLE	1.41×10^{11}	NOT AVAILABLE	$3.39 \times 10^{[illegible]}$	50×10^{-6}	17.5×10^{-6}	1.43×10^{4}	2.02×10^{15}	[illegible]
NOT AVAILABLE	NOT AVAILABLE	NOT AVAILABLE	NOT AVAILABLE	NOT AVAILABLE	$50 \times 10^{-}$	$17.5 \times 10^{-}$	1.43×10^{4}	NOT AVAILABLE	NOT AVAIL
4.05×10^{12}	4.81×10^{12}	8.34×10^{12}	1.57×10^{10}	2.01×10^{4}	50×10^{-6}	17.5×10^{-6}	1.43×10^{4}	1.19×10^{17}	2.31 x 10
4.05×10^{12}	4.81×10^{12}	8.34×10^{12}	1.57×10^{10}	2.01×10^{4}	50×10^{-6}	17.5×10^{-6}	1.43×10^{4}	1.19×10^{17}	2.31 x 10
3.42×10^{12}	4.05×10^{12}	4.94×10^{12}	1.41×10^{1}	1.19×10^{4}	$50 \times 10^{-}$	17.5×10^{-6}	1.43×10^{4}	7.06×10^{16}	1.49 x 10
NOT AVAILABLE	NOT AVAILABLE	7.03×10^{10}	NOT AVAILABLE	$1.69 \times 10^{[illegible]}$	$50 \times 10^{-}$	17.5×10^{-6}	1.43×10^{4}	1.01×10^{15}	3.8×10^{1}
NOT AVAILABLE	NOT AVAILABLE	NOT AVAILABLE	NOT AVAILABLE	NOT AVAILABLE	50×10^{-6}	17.5×10^{-6}	1.43×10^{4}	NOT AVAILABLE	NOT AVAIL.
3.42×10^{12}	4.05×10^{12}	7.03×10^{12}	1.41×10^{10}	1.69×10^{4}	50×10^{-6}	17.5×10^{-6}	1.43×10^{4}	1.01×10^{17}	2.15 x 10
3.42×10^{12}	4.05×10^{12}	7.03×10^{12}	1.41×10^{10}	1.69×10^{4}	50×10^{-6}	17.5×10^{-6}	1.43×10^{4}	1.01×10^{17}	2.15 x 10
4.08×10^{12}	4.85×10^{12}	$5.1[illegible] \times 10^{12}$	1.47×10^{10}	$1.2[illegible] \times 10^{4}$	$52 \times 10^{-}$	18.2×10^{-6}	1.37×10^{4}	6.99×10^{16}	1.44 x 10
NOT AVAILABLE	NOT AVAILABLE	7.79×10^{10}	NOT AVAILABLE	1.88×10	$52 \times 10^{-}$	18.2×10^{-6}	1.37×10^{4}	1.07×10^{15}	3.6×10^{1}
NOT AVAILABLE	NOT AVAILABLE	NOT AVAILABLE	NOT AVAILABLE	NOT AVAILABLE	$52 \times 10^{-}$	18.2×10^{-6}	1.37×10^{4}	NOT AVAILABLE	NOT AVAIL
4.08×10^{12}	4.85×10^{12}	8.41×10^{1}	1.47×10^{10}	2.03×10^{4}	$52 \times 10^{-}$	18.2×10^{-6}	1.37×10^{4}	1.15×10^{17}	2.29×10^{3}
4.08×10^{12}	4.85×10^{12}	8.41×10^{12}	1.47×10^{10}	[illegible] $\times 10^{4}$	52×10^{-6}	18.2×10^{-6}	1.37×10^{4}	1.15×10^{17}	2.29×10^{3}
2.89×10^{12}	3.32×10^{12}	5.58×10^{1}	1.22×10^{1}	1.34×10^{4}	$52 \times 10^{-}$	18.2×10^{-6}	1.37×10^{4}	7.64×10^{16}	1.77×10^{3}
2.89×10^{12}	3.32×10^{12}	5.07×10^{12}	1.22×10^{10}	1.22×10^{4}	52×10^{-6}	18.2 x 10-6	1.37×10^{4}	6.95×10^{16}	2.88×10^{3}
NOT AVAILABLE	NOT AVAILABLE	NOT AVAILABLE	NOT AVAILABLE	NOT AVAILABLE	52×10^{-6}	18.2×10^{-6}	1.37×10^{4}	NOT AVAILABLE	NOT AVAILA
2.89×10^{12}	3.32×10^{12}	3.68×10^{12}	1.22×10^{10}	8.85×10^{3}	$52 \times 10^{-}$	18.2×10^{-6}	1.37×10^{4}	5.04×10^{16}	1.74×10^{3}
2.89×10^{12}	3.32×10^{12}	5.58×10^{12}	1.22×10^{10}	1.34×10^{4}	52×10^{-6}	18.2×10^{-6}	1.37×10^{4}	7.64×10^{16}	1.77×10^{3}
2.89×10^{12}	3.32×10^{12}	5.58×10^{12}	1.22×10^{10}	1.34×10^{4}	52×10^{-6}	18.2×10^{-6}	1.37×10^{4}	7.64×10^{16}	1.77×10^{3}
2.89×10^{12}	3.32×10^{12}	5.59×10^{12}	1.21×10^{10}	1.34×10^{4}	50×10^{-6}	17.5×10^{-6}	1.43×10^{4}	[illegible] $\times 10^{16}$	2.47×10^{3}
2.89×10^{12}	3.32×10^{12}	4.78×10^{12}	1.21×10^{10}	1.15×10^{4}	50×10^{-6}	17.5×10^{-6}	1.43×10^{4}	6.84×10^{16}	2.83×10^{3}
NOT AVAILABLE	NOT AVAILABLE	NOT AVAILABLE	NOT AVAILABLE	NOT AVAILABLE	50×10^{-6}	17.5×10^{-6}	1.43 x 1		NOT AVAILA
2.89×10^{12}	3.32×10^{12}	3.90×10^{12}	1.21×10^{10}	9.40×10^{3}	50×10^{-6}	17.5×10^{-6}	1.43 x 1		1.62×10^{3}
2.89×10^{12}	3.32×10^{12}	5.59×10^{12}	1.21×10^{10}	1.34×10^{4}	50×10^{-6}	17.5×10^{-6}	1.43 x 1		2.47×10^{3}
2.89×10^{12}	3.32×10^{12}	5.59×10^{12}	1.21×10^{10}	1.34×10^{4}	50×10^{-6}	17.5×10^{-6}	1.43 x 1		2.47 x 103

TABLE 11. NEUTRON AND γ - RAY DOSIMETRY PROVINDING INTEGRAL DOSE AND DOSE RATE EXPOSURES TO THE MICROWAVE COMPONENTS

(SHEET 2)

	12	13	14	15	16	17	18
FUR[dt] I ET	PULSE WIDTH AT HALF-MAX. DETERMINED FROM SPRF PHOTOGRAPH, SEC.	τ $\frac{\text{PULSE WIDTH}}{2.86}$ REACTOR PERIOD, SEC	$1/4\tau$ F_{MAX}/F_{TOTAL}	$F_m/F_t \int \phi E_n > 10$ kev[dt] PEAK INCIDENT NEUTRON FLUX (NEUTRON/cm^2 SEC.)	INTEGRATED GAMMA DOSE, RADS (H_2O)	$1.07 \times 10^3 D_n$ PEAK INCIDENT GAMMA DOSE RADS/SEC.	RADIATION EFFECT ON COMPONENT
	50×10^{-6}	17.5×10^{-6}	1.43×10^4	9.15×10^{16}	2.63×10^3	1.65×10^7	0.047 DB INCREASE IN INSERTION LOSS OF PRIMARY CIRCULATOR 1.000 DB INCREASE IN ISOLATION OF PRIMARY CIRCULATOR
	50×10^{-6}	17.5×10^{-6}	1.43×10^4	6.61×10^{16}	2.79×10^3	1.19×10^7	0.060 DB INCREASE IN INSERTION LOSS OF DEVICE 0.017 DB CHANGE IN VSWR SIGNAL ~ 1.46 DB INCREASE IN INSERTION LOSS OF CIRCULATOR
	50×10^{-6}	17.5×10^{-6}	1.43×10^4	9.97×10^{16}	3.12×10^3	1.80×10^7	~ 0.637 DB INCREASE IN ISOLATION
	50×10^{-6}	17.5×10^{-6}	1.43×10^4	9.37×10^{16}	2.72×10^3	1.69×10^7	20.3×10^6 Ω APPARENT RESISTANCE ACROSS COMPONENT
	50×10^{-6}	17.5×10^{-6}	1.43×10^4	9.37×10^{16}	2.72×10^3	1.69×10^7	174×10^6 Ω APPARENT RESISTANCE ACROSS COMPONENT
	50×10^{-6}	17.5×10^{-6}	1.43×10^4	7.79×10^{16}	1.72×10^3	1.40×10^7	0.040 DB CHANGE IN VSWR SIGNAL
	50×10^{-6}	17.5×10^{-6}	1.43×10^4	1.10×10^{17}	2.24×10^3	1.97×10^7	0.208 DB INCREASE IN INSERTION LOSS
	50×10^{-6}	17.5×10^{-6}	1.43×10^4	NOT AVAILABLE	NOT AVAILABLE	NOT AVAILABLE	[illegible].765 DB INCREASE IN INSERTION LOSS
	50×10^{-6}	17.5×10^{-6}	1.43×10^4	1.10×10^{17}	2.34×10^3	1.99×10^7	19.2×10^6 Ω APPARENT RESISTANCE ACROSS COMPONENT
	50×10^{-6}	17.5×10^{-6}	1.43×10^4	1.10×10^{17}	2.34×10^3	1.99×10^7	153×10^7 Ω APPARENT RESISTANCE ACROSS COMPONENT
	50×10^{-6}	17.5×10^{-6}	1.43×10^4	7.15×10^{16}	1.64×10^3	1.28×10^7	0.051 DB INCREASE IN INSERTION LOSS OF PRIMARY CIRCULATOR 0.050 DB CHANGE IN VSWR SIGNAL
	50×10^{-6}	17.5×10^{-6}	1.43×10^4	5.05×10^{15}	$1.27 \times 10^{[illegible]}$	9.10×10^5	0.018 INCREASE IN INSERTION LOSS
	50×10^{-6}	17.5×10^{-6}	1.43×10^4	NOT AVAILABLE	NOT AVAILABLE	NOT AVAILABLE	~ 0.445 DB INCREASE IN INSERTION LOSS
	50×10^{-6}	17.5×10^{-6}	1.43×10^4	9.61×10^{16}	2.31×10^3	1.73×10^7	27.5×10^6 Ω APPARENT RESISTANCE ACROSS COMPONENT
	50×10^{-6}	17.5×10^{-6}	1.43×10^4	9.61×10^{16}	2.31×10^3	1.73×10^7	93.[illegible] $\times 10^7$ Ω APPARENT RESISTANCE ACROSS COMPONENT
	50×10^{-6}	17.5×10^{-6}	1.43×10^4	7.28×10^{16}	[illegible]	[illegible]	0.060 DB INCREASE IN INSERTION LOSS OF PRIMARY CIRCULATOR 0.056 DB CHANGE IN VSWR SIGNAL
	50×10^{-6}	17.5×10^{-6}	1.43×10^4	2.02×10^{15}	[illegible]	[illegible]	[illegible].18 DB INCREASE IN INSERTION LOSS
	50×10^{-6}	17.5×10^{-6}	1.43×10^4	NOT AVAILABLE	NOT AVAILABLE	NOT AVAILABLE	[illegible] DB DECREASE IN INSERTION LOSS
	50×10^{-6}	17.5×10^{-6}	1.43×10^4	1.19×10^{17}	2.31×10^3	2.15×10^7	25.6×10^6 APPARENT RESISTANCE ACROSS COMPONENT
	50×10^{-6}	17.5×10^{-6}	1.43×10^4	1.19×10^{17}	2.31×10^3	2.15×10^7	108×10^7 APPARENT RESISTANCE ACROSS COMPONENT
	50×10^{-6}	17.5×10^{-6}	1.43×10^4	7.06×10^{16}	1.49×10^3	1.27×10^7	0.048 DB INCREASE IN INSERTION LOSS
	50×10^{-6}	17.5×10^{-6}	1.43×10^4	1.01×10^{15}	3.8×10^1	1.81×10^5	NONE OBSERVED
	50×10^{-6}	17.5×10^{-6}	1.43×10^4	NOT AVAILABLE	NOT AVAILABLE	NOT AVAILABLE	0.095 DB INCREASE IN CIRCULATOR INSERTION LOSS
	50×10^{-6}	17.5×10^{-6}	1.43×10^4	1.01×10^{17}	2.15×10^3	1.81×10^7	306×10^7 APPARENT RESISTANCE ACROSS COMPONENT
	50×10^{-6}	17.5×10^{-6}	1.43×10^4	1.01×10^{17}	2.15×10^3	1.81×10^7	81.7×10^6 APPARENT RESISTANCE ACROSS COMPONENT
	52×10^{-6}	18.2×10^{-6}	1.37×10^4	6.99×10^{16}	1.44×10^3	1.32×10^7	0.049 DB INCREASE IN INSERTION LOSS
	52×10^{-6}	18.2×10^{-6}	1.37×10^4	1.07×10^{15}	3.6×10^1	2.01×10^5	0.012 DB INCREASE IN INSERTION LOSS
	52×10^{-6}	18.2×10^{-6}	1.37×10^4	NOT AVAILABLE	NOT AVAILABLE	NOT AVAILABLE	0.143 DB INCREASE IN CIRCULATOR INSERTION LOSS
	52×10^{-6}	18.2×10^{-6}	1.37×10^4	1.15×10^{17}	2.29×10^3	2.17×10^7	77.1×10^6 APPARENT RESISTANCE ACROSS COMPONENT
	52×10^{-6}	18.2×10^{-6}	1.37×10^4	1.15×10^{17}	2.29×10^3	2.17×10^7	198×10^7 APPARENT RESISTANCE ACROSS COMPONENT
	52×10^{-6}	18.2×10^{-6}	1.37×10^4	7.64×10^{16}	1.77×10^3	1.43×10^7	0.044 DB INCREASE IN INSERTION LOSS 0.091 DB INCREASE IN ISOLATION
	52×10^{-6}	18.2×10^{-6}	1.37×10^4	6.95×10^{16}	2.88×10^3	1.31×10^7	0.041 DB INCREASE IN INSERTION LOSS OF CIRCULATOR
	52×10^{-6}	18.2×10^{-6}	1.37×10^4	NOT AVAILABLE	NOT AVAILABLE	NOT AVAILABLE	NONE OBSERVED
	52×10^{-6}	18.2×10^{-6}	1.37×10^4	5.04×10^{16}	1.74×10^3	9.47×10^6	~ 1.052 DB INCREASE IN INSERTION LOSS
	52×10^{-6}	18.2×10^{-6}	1.37×10^4	7.64×10^{16}	1.77×10^3	1.43×10^7	262×10^6 Ω APPARENT RESISTANCE ACROSS COMPONENT
	52×10^{-6}	18.2×10^{-6}	1.37×10^4	7.64×10^{16}	1.77×10^3	1.43×10^7	47.7×10^6 APPARENT RESISTANCE ACROSS COMPONENT
	50×10^{-6}	17.5×10^{-6}	1.43×10^4	[illegible].06 $\times 10^{16}$	2.47×10^3	1.43×10^7	[illegible].055 DB INCREASE IN INSERTION LOSS 0.057 DB INCREASE IN ISOLATION
	50×10^{-6}	17.5×10^{-6}	1.43×10^4	6.84×10^{16}	2.88×10^3	1.23×10^7	0.066 DB INCREASE IN INSERTION LOSS OF CIRCULATOR 0.020 DB INCREASE IN INSERTION LOFF OF DEVICE
	50×10^{-6}	17.5×10^{-6}	1.43×10^4	NOT AVAILABLE	NOT AVAILABLE	NOT AVAILABLE	~ - 1.302 DB DECREASE IN INSERTION LOSS OF FRONT END
	50×10^{-6}	17.5×10^{-6}	1.43×10^4	5.58×10^{16}	1.62×10^3	1.01×10^7	NONE OBSERVED
	50×10^{-6}	17.5×10^{-6}	1.43×10^4	8.00×10^{16}	2.47×10^3	1.43×10^7	234×10^6 Ω APPARENT RESISTANCE ACROSS COMPONENT
	50×10^{-6}	17.5×10^{-6}	1.43×10^4	8.00×10^{16}	2.47×10^3	1.43×10^7	39.6 APPARENT RESISTANCE ACROSS COMPONENT

* In dc experiments voltage across components is indicated in volts and polarities are shown.

FOR OFFICIAL USE ONLY

3

5. CONCLUSIONS

The following conclusions are based on operation of the C-band microwave components at power levels of 80-160 milliwatts in the frequency range of 5.4 to 5.9 Gc and in a radiation environment of the content and duration of that produced during a burst at the SPRF. The limits of the radiation effects on the operating characteristics of the components are the following:

- C-band coaxial ferrite Y-junction circulator - The average transient increase in the insertion loss of the circulator is less than 10 per cent, i.e. less than 0.05 db. The average transient increase in the isolation of the circulator is less than 0.5 per cent, i.e. less than 0.10 db.

- Internal magnet coaxial isolator - The average transient increase in insertion loss of the isolator operating in the forward direction is less than 15 per cent, i.e. less than 0.15 db. The average transient increase in isolation of the isolator operating in the reverse direction is less than 1 per cent, i.e. less than 0.07 db.

- Gyromagnetic coupling limiter - The average transient increase in the insertion loss of the limiter is less than 10 per cent, i.e. less than 0.11 db.

For operation at a power level of 800 milliwatts, wherein 200 milliwatts is the point at which power limiting begins, the average transient increase in insertion loss of the limiter is less than 85 per cent, i.e. less than 0.85 db.

Tests of C-band brass and aluminum waveguide elements with air, high density Styrofoam and low density Styrofoam dielectrics indicate that significant transient increases in attenuation occur at the time of the burst. The results of these measurements are presented briefly in the following table.

TABLE 12

RESULTS OF PULSED RADIATION ENVIRONMENT TESTS ON MICROWAVE RECTANGULAR WAVEGUIDES

Test Element	Inherent Attenuation Per Foot @ 5.6 Gc, db	Magnitude Of Transient Increase In Attenuation During Radiation Burst Per Foot, (Experimental Value) db	Per Cent Increase In Attenuation Due To Radiation
BRASS WAVEGUIDE WITH AIR DIELECTRIC	0.015 [c]	0.35	2300
ALUMINUM WAVEGUIDE WITH AIR DIELECTRIC	0.012 [c]	0.27	2250
BRASS WAVEGUIDE WITH LOW DENSITY [a] STYROFOAM DIELECTRIC	~0.09 [d]	0.92	1000
ALUMINUM WAVEGUIDE WITH LOW DENSITY [a] STYROFOAM DIELECTRIC	~0.09 [d]	0.70	780
BRASS WAVEGUIDE WITH HIGH DENSITY [b] STYROFOAM DIELECTRIC	~0.09 [d]	0.10	110
ALUMINUM WAVEGUIDE WITH HIGH DENSITY [b] STYROFOAM DIELECTRIC	~0.09 [d]	0.09	100

[a] LOW DENSITY STYROFOAM: ρ = 1.6 - 2.0 lbs./ft.^{3}

[b] HIGH DENSITY STYROFOAM: ρ = 4.0 - 4.7 lbs./ft.^{3}

[c] VALUES OBTAINED FROM LITERATURE

[d] CALCULATED VALUES

Placement of the front end inside the KIVA, in an attempt to deliver more power to the components, resulted in somewhat inconsistent data indicating that this method of obtaining higher power operation is not very satisfactory.

The significance of these conclusions to the microwave equipment designer is the following:

- If possible, the use of coaxial dielectric (other than air) and/or ferrite filled microwave components in a radiation environment is more desirable than the use of waveguide air dielectric microwave components. For operating powers of 150 milliwatts or less, the circulator, limiter and isolator will function satisfactorially during exposure to radiation bursts such as those described in Table 11.

The significance of these conclusions to the microwave tube designer is the following:

- The klystron (Varian Model X-26F), which was placed inside the KIVA, showed no signs of permanent damage or degradation; however, transient decreases in signal power level did occur. These decreases may have been caused by changes in the reflector voltage characteristics due to external leakage.

The significance of these conclusions to individuals engaged in the study of radiation damage mechanisms is the following:

- The radiation effects in both the brass and aluminum waveguide elements, with air as the dielectric, are intermediate in magnitude to the effects with the high density Styrofoam dielectric (less effect) in each waveguide and the effects with the low density Styrofoam dielectric (greater effect) in each waveguide. At present this difference in magnitudes is difficult to understand and the following explanation is regarded as only a possibility.

Assume electrons are emitted from the waveguide walls due to Compton collisions of the γ-rays with the atoms in the walls. These electrons cause ionization in the dielectric, wherein the degree of ionization is assumed to be proportional to the increase in attenuation. If the gas in the Styrofoam, methyl chloride, is more susceptible to electron caused ionization than air, then it is reasonable to believe that the use of the low density Styrofoam dielectric should result in effects of larger magnitude than those observed for the air dielectric. The mean free path of the Compton electrons may be significantly shorter in the high density Styrofoam than in the low density Styrofoam. The high density Styrofoam would then attenuate the electrons before they reached the high electric field intensity central portion of the waveguide. Thus, even though ionization might occur in the high density Styrofoam it would not occur in the important high electric field intensity portion of the waveguide. The signal attenuation would thus not be as pronounced as that observed for the low density Styrofoam dielectric filled waveguide.

6. REFERENCES

1. Private communication with A. Hinchee and G. R. Barton.

2. Harrison, G. R. and Scheiwe, J. P., "Study of Pulsed Radiation Effects on Microwave Ferrite Duplexers", Report No. 1 Contract No. DA 36-039-SC-89113, First quarterly Report, Sperry Microwave Electronics Co., pp 4-31 to 4-41.

3. Harrison, G. R. and Scheiwe, J. P., "Study of Pulsed Radiation Effects on Microwave Ferrite Duplexers", Report No. 2 Contract No. DA 36-039-SC-89113, Second quarterly Report, Sperry Microwave Electronics Co., pp 4-1 to 4-51.

4. ibid., p 4-21.

5. ibid., p 4-23.

6. ibid., pp 4-28 and 4-29.

7. Torrey, H. C. and Whitmer, C. A., "Crystal Rectifiers", McGraw-Hill Book Co., Inc., 1948, p 3.

8. Westman, H. P. (editor), "Reference Data for Radio Engineers", International Telephone and Telegraph Corp., 1962, p 615.

9. Saad, T. S. (editor), "The Microwave Engineers" Handbook", Horizon House-Microwave Inc., 1963, p T-28.

10. Harrison, G. R. and Scheiwe, J. P., "Study of Pulsed Radiation Effects on Microwave Ferrite Duplexers", Report No. 2 Contract No. DA 36-039-SC-89113, Second Quarterly Report, Sperry Microwave Electronics Co., p 4-32.

11. ibid., p 4-39.

12. Private communication with P. D. O'Brien.

13. Private communication with L. L. Flores.

14. Plankis, E. P., "Radiation Effects on Microwave Devices", Report No. 3 Contract No. DA-36-039-SC-87253, Third Quarterly Progress Report, General Electric Co., Power Tube Department, p 69 and p 73.

7. PROGRAM FOR NEXT INTERVAL

(1 February 1963 to 30 April 1963)

The third series of experiments, scheduled for the week of May 13, 1963, will be planned. Since some of these experiments will be performed on waveguide duplexing devices, some modifications in the present measurement scheme may be required. These modifications will be made and the new measurement scheme will be "dry run" at Sperry Microwave Electronics Company.

8. IDENTIFICATION OF PERSONNEL

During the quarter (1 November 1962 to 31 January 1963) 829.5 engineering man hours were devoted to this contract by the personnel listed below. A brief biography of Mr. R. W. Coston appears on the following page. Biographies of the other personnel appear in the first two quarterly reports.

B. J. Duncan	21.0 hours
E. W. Matthews	22.0 hours
G. R. Harrison	159.0 hours
J. C. Hoover	52.5 hours
G. R. Barton	5.0 hours
A. E. Hinchee	44.0 hours
R. W. Coston	132.0 hours
J. P. Scheiwe	394.0 hours

R. W. COSTON, Engineer

Professional Experience

- Research and development of TE_{01} circulator waveguide devices including duplexers, isolators, phase shifters, and variable attenuators

- Research and development of a Zero Permeability Duplexer

- Research and development of a High Power Variable Attenuator

- Development of a High Speed Ferrite Switch

- Instruction and Supervision of Military personnel in Airborne and Ground Radar and associated electronics.

REVISED DISTRIBUTION LIST

Contract DA 36-039 SC-89113	No. of Copies
OASD (R&E) Attn: Technical Library Rm. 3E1065, The Pentagon Washington 25, D. C.	1
Commander Armed Services Technical Information Agency Attn: TISIA Arlington Hall Station Arlington 12, Virginia	20
Advisory Group on Electron Devices 346 Broadway New York 13, New York	2
Director U. S. Naval Research Laboratory Attn: Code 2027 Washington 25, D.C.	1
Commanding Officer & Director U. S. Navy Electronics Laboratory San Diego 52, California	1
Chief, Bureau of Ships Department of the Navy Attn: 681A-1 Washington 25, D. C.	1
Commander Aeronautical Systems Division Attn: ASAPRL Wright-Patterson AFB, Ohio	1
Commander, AF Cambridge Research Laboratories Attn: CRZC (1 cy) L. G. Hanscom Field Bedford, Massachusetts	1
Commander Air Force Cambridge Research Laboratory Attn: CRXL-R, Research Library L. G. Hanscom Field Bedford, Massachusetts	1

	No. of Copies
Commander Rome Air Development Center Attn: RAALD Griffiss Air Force Base, New York	1
AFSC Scientific/Technical Liaison Office U. S. Naval Air Development Center Johnsville, Pennsylvania	1
Chief of Research and Development Department of the Army Washington 25, D. C.	1
Chief, U. S. Army Security Agency Arlington Hall Station Arlington 12, Virginia	2
Deputy President U. S. Army Security Agency Board Arlington Hall Station Arlington 12, Virginia	1
Commanding Officer U. S. Army Electronics Research Unit P. O. Box 205 Mountain View, California	1
Commanding Officer Harry Diamond Laboratories Connecticut Avenue & Van Ness Street, N. W. Washington 25, D. C. Attn: Library, Rm. 211, Bldg. 92	1
Commander U. S. Army Missile Command Attn: Technical Library Redstone Arsenal, Alabama	1
Commanding Officer U. S. Army Electronics Command Attn: AMSEL-AD Fort Monmouth, New Jersey	3
Commanding Officer U. S. Army Electronics Materiel Support Agency Attn: SELMS-ADJ Fort Monmouth, New Jersey	1
Corps of Engineers Liaison Office U. S. Army Electronics R & D Laboratory Fort Monmouth, New Jersey	1

No of Copies

Marine Corps Liaison Officer
U. S. Army Electronics R & D Laboratory
Attn: SELRA/LNR
Fort Monmouth, New Jersey — 1

Commanding Officer
U. S. Army Electronics R & D Laboratory
Attn: Director of Research
Fort Monmouth, New Jersey — 1

Commanding Officer
U. S. Army Electronics R & D Laboratory
Attn: Technical Documents Center
Fort Monmouth, New Jersey — 1

Commanding Officer
U. S. Army Electronics R & D Laboratory
Attn: SELRA/PR (Contracts) (1 cy)
SELRA/PR (Tech Staff) (1 cy)
SELRA/PRG (Mr. Zinn) (1 cy)
SELRA/PRM (Mr. Hersh) (1 cy)
Fort Monmouth, New Jersey — 4

Commanding Officer
U. S. Army Electronics R & D Laboratory
Attn: Logistics Division (For: SELRA/PRT Project Engineer)
Fort Monmouth, New Jersey — 1

Commanding Officer
U. S. Army Electronics R & D Laboratory
Attn: SELRA/PRT, Record File Copy
Fort Monmouth, New Jersey — 1

Commanding General
U. S. Army Materiel Command
Attn: R & D Directorate
Washington 25, D. C. — 1

Commanding General
U. S. Army Combat Developments Command
Attn: CDCMR-E
Fort Belvoir, Virginia — 1

No. of Copies

Commanding Officer U. S. Army Combat Developments Command Communications & Electronics Agency Fort Huachuca, Arizona	1
Hq., Electronic Systems Division Attn: ESAT L. G. Hanscom Field Bedford, Massachusetts	1
Director, Monmouth Office U. S. Army Combat Developments Command Communications-Electronics Agency, Bldg. 410 Fort Monmouth, New Jersey	1
AFSC Scientific/Technical Liaison Office U. S. Army Electronics R & D Laboratory Fort Monmouth, New Jersey	1
USAELRDL Liaison Office Rome Air Development Center Attn: RAOL Griffiss Air Force Base, New York	1
Commanding Officer U. S. Army Electronics Materiel Agency Attn: SELMA-R2a 225 South 18th Street Philadelphia, Pennsylvania	1
Commander Aeronautical Systems Division Attn: ASRNET Wright-Patterson Air Force Base, Ohio	1
Defense Atomic Support Agency Attn: Major Ralph I. LaRock, DASA RA-4 Washington 25, D. C.	1
Commander, Field Command Defense Atomic Support Agency Attn: FCWT (1 cy) Attn: SPRF Coordinator (1 cy) Sandia Base Alburquerque, New Mexico	2

No. of Copies

Radiation Effects Information Center Battelle Memorial Institute 505 King Avenue Columbus 1, Ohio Attn: Mr. D. C. Jones	1
Chief of Research and Development Department of the Army Washington 25, D. C. Attn: Atomics Division, Major D. Baker	1
U. S. Army Air Defense School Fort Bliss, Texas Attn: AKBAAS-CD-R	1
Commanding Officer Harry Diamond Laboratories Connecticut Avenue & Van Ness Street, N. W. Washington 25, D. C. Attn: Chief, Nuclear Vulnerability Branch (230) Attn: Technical Library (011)	 1 1
Chief, Bureau of Naval Weapons Navy Department, Special Projects Office Washington 25, D. C. Attn: SP-2721 (Mr. D. R. Williams)	1
Applied Physics Laboratory The John Hopkins University 8621 Georgia Avenue Silver Spring, Maryland Attn: Mr. Robert Freiberg (For BuWeps RMGA-4)	1
U. S. Atomic Energy Commission Office of Technical Information Extension P. O. Box 62 Oak Ridge, Tennessee	3
Hughes Aircraft Company Ground systems Group 1901 W. Malvern Avenue Fullerton, California Attn: T. D. Hanscome MS 393/B122	1

No. of Copies

General Atomic P. O. Box S, Old San Diego Station San Diego, California Attn: Dr. V. A. J. van Lint	1
Northrup Corporation Radioplane Division 8000 Woodley Avenue Van Nuys, California Attn: Dr. D. A. Hicks	1
ARINC Research Corporation 1700 K Street, N. W. Washington 6, D. C. Attn: Mr. William H. Van Alven	1
Commanding Officer Naval Ordnance Laboratory Corona, California Attn: Dr. Bryant	1
Commander Naval Ordnance Laboratory, White Oak Silver Spring, Maryland Attn: Mr. Grantham	1
Commander U. S. Naval Material Laboratory New York Naval Shipyard, Naval Base Brooklyn 1, New York	1
Commanding Officer and Director U.S. Naval Radiological Defense Laboratory San Francisco 24, California	1
President, Sandia Corporation Sandia Base Albuquerque, New Mexico	
Attn: Dr. J. W. Easley, 5300	1
Attn: A. W. Snyder, 5313	1
Attn: Carter Broyles, 5113	1
Director Advanced Research Projects Agency Washington 25, D. C. Attn: Lt Col W. H. Innes	1

	No. of Copies
Admiral Corporation 3800 Cortland Street Chicago 47, Illinois Attn: Mr. R. Whitner	1
North American Aviation Corporation Atomics International Division 21600 Van Owen Street Canoga Park, California Attn: Dr. A. Saur	1
Burroughs Corporation Central Avenue & Route 202 Paoli, Pennsylvania	1
General Dynamics/Fort Worth Convair Division, Grants Lane Fort Worth 1, Texas Attn: Mr. E. L. Burkhard	1
General Electric Company Power Tube Department, Bldg 269 1 River Road Schenectady, New York Attn: Mr. David Hodges	1
Stevens Institute of Technology 501 and 711 Hudson Street Hoboken, New Jersey Attn: E. J. Henley	1
Commanding Officer U. S. Army Combat Developments Command, Nuclear Group Fort Bliss, Texas Attn: Major Doerflinger	1
Chief, Bureau of Naval Weapons Navy Department Washington 25, D. C. Attn: RMGA-8 Attn: RRNV	 1 1
Chief, Bureau of Ships Navy Department Washington 25, D. C. Attn: Code 362B	2

No. of Copies

USAF Project RAND, Via AF Liaison Office The RAND Corporation 1700 Main Street Santa Monica, California Attn: Mr. J. Whitener	1
Chief, Defense Atomic Support Agency Washington 25, D. C, Attn: Document Library Branch	1
Georgia Institute of Technology and Engineering Experiment Station 722 Cherry Street, N. W. Atlanta 13, Georgia Attn: Dr. R. B. Belser	1
Hughes Aircraft Company Florence and Teale Streets Culver City, California Attn: Dr. C. Perkins	1
International Business Machine Corporation Federal Systems Division Route 17C Owego, New York Attn: Mr. Bohan	1
Space Technology Laboratories 5730 Arbor Vitae Street Los Angeles, California Attn: Dr. B. Sushols, Mr. J. Maxey THRU: DCAS, AF Unit Post Office Los Angeles, California Attn: TDC 61-1019-4	1
Chief of Naval Operations Navy Department Washington 25, D.C. Attn: OP 754	1
The Boeing Company, Aerospace Division Physics Technology Department 7755 E. Marginal Way Seattle 8, Washington Attn: Dr. Glenn Keister	1

No. of Copies

General Electric Company
316 E. Ninth Street
Owensboro, Kentucky
Attn: Mr. Daniel D. Mickey, Receiving Tube Department 1

Commanding Officer
U. S. Army Electronics R & D Laboratory
Fort Monmouth, New Jersey
Attn: SEIRA/PEM (Mr. I. Bady) 1
Attn: SEIRA/PEM (Mr. Nat Lipetz) 1
Attn: SEIRA/PRM (Mr. W. H. Wright) 1

Chief of Naval Research, Navy Department
Washington 25, D. C.
Attn: Code 418 1
Attn: Code 427 1

HQ, USAF (AFCIN), Washington 25, D. C. 1

HQ, USAF (AFTAC), Washington 25, D. C. 1

HQ, USAF (AFRDC/NE), Washington 25, D. C. 1

ADC (ADOOP), Ent AFB, Colorado 1

SAC (OAWS) Offutt AFB, Nebraska 1

TAC (TPL-RQD-M) Langley AFB, Virginia 1

HQ, R&T Division
(RTW) Bolling AFB
Washington 25, D. C. 1

AFSC (SCR, DCS/R&E) Andrews AFB, Md 1

HQ, AFSWC
Kirtland AFB, New Mexico
Attn: SWOI 1
Attn: SWRPA (Capt. Glenn) 1
Attn: SWRPL 1

Commanding Officer
Naval Weapons Evaluation Facility
Kirtland AFB, New Mexico
Attn: Code 3434 1

APGC (PGAPI) Eglin AFB, Fla 1

	No. of Copies
Brookhaven National Laboratory Associated Universities Inc. Upton, Long Island, New York Attn: Dr. G. H. Vineyard	1
Bell Telephone Laboratories, Inc Whippany Road Whippany, New Jersey Attn: U. S. Army Materiel Command Liaison Officer	1
General Electric Company Radiation Effects Operations Syracuse, New York Attn: Mr. Edward H. Brooks	1
General Electric Company Radiation Effects Operations Defense Systems Department 300 South Geddes Street Syracuse, New York Attn: Mr. L. Dee	1
Lockheed Aircraft Corporation Missile and Space Division 1111 Lockheed Way Sunnyvale, California Attn: Mr. Fred Barline, Dept 5872	1
New York University Washington Square New York 3, New York Attn: Mr. H. Kallmann, Physics Dept.	1
North American Aviation Corporation Atomics International Division 8900 De Soto Street Canoga,Park, California Attn: W. E. Parkins, Mgr. of Research	1

No. of Copies

Procedyne Associates, Inc. 376 Ridgey Street Perth Amboy, New Jersey Attn: Dr. R. Staffin	1
Radio Corporation of America New Holland Pike Lancaster, Pennsylvania Attn: Mr. Herman A. Stern	1
Raytheon Company 55 Chapel Street Newton, Massachusetts Attn: Mr. Francis J. Barry	1
Sperry Gyroscope Company Division of Sperry Rand Corporation Great Neck, New York Attn: Mr. J. Rogers (Mail Stop 1A36)	1
Sylvania Electric Products, Inc. 1891 East 3rd Street Williamsport, Pennsylvania Attn: Mr. John H. O'Neill, Microwave Devices Division	1
Tung-Sol Electric, Inc. 200 Bloomfield Avenue Bloomfield, New Jersey Attn: Mr. Max Bareiss	1
Westinghouse Electric Corporation P. O. Box 284 Elmira, New York Attn: Mr. Edmund L. Dana, Jr.	1

This contract is supervised by the Techniques Branch, Electron Tubes Division, ECD, USAEIRDL, Fort Monmouth, New Jersey. For further technical information contact Mr. Willis A. Dworzak, Project Engineer, Telephone 201-59-61581.

AD Div. 8/4, 14/11, 17/9

Sperry Microwave Electronics Company, Division of Sperry Rand Corporation, Clearwater, Florida.
STUDY OF PULSED RADIATION EFFECTS ON MICROWAVE FERRITE DUPLEXERS. By J. P. Scheiwe, G. R. Harrison. Third Quarterly Report - 1 November 1962 to 31 January 1963. [illegible] pp Inc. Illus-Graphs, 14 refs. (Rept. No. SJ-222-004-3)

Contract DA36-039-SC-89113 Unclassified Report

This report presents the results from the second series of radiation environment experiments conducted during the third quarter of the program. These experiments were performed to substantiate and extend the data on the duplexer components' behavior obtained during the first series of experiments. Data are also presented from preliminary investigations of the radiation effects in waveguide elements (which might be required for future high power tests) and static dc voltage experiments which were conducted to simulate possible high microwave power electric field intensities.

Briefly described and reviewed are procedures for testing the coaxial ferrite Y-junction circulator, the gyromagnetic coupling limiter, the internal magnet coaxial isolator and C-band waveguide elements at a microwave power of 100 milliwatts in the frequency range of 5.4 to 5.9 Gc. Also reviewed is the method used to perform the static dc voltage experiments involving tests of the microwave components mentioned above, various open ended connectors (potted and unpotted) and short pieces of open ended cable.

Photographs of oscilloscope traces showing radiation effects on the operating characteristics of the microwave components and leakage characteristics of the components used in the dc experiments are presented. Quantitative interpretations of the data obtained by circuit calibration procedures are also presented.

Results of dosimetry provided by the SPRF are tabulated along with the radiation effects noted in the components investigated in each experiment.

UNCLASSIFIED

1. Pulsed Radiation Effects in Ferrite Duplexers
2. Duplexers, C-Band
3. Circulator, ferrite
4. Gyromagnetic coupling ferrite limiter
5. Isolator, ferrite

I. Radiation effects
II. Scheiwe, J. P.
III. Harrison, G. R.
IV. U. S. Army Electronics R&D Laboratory, Ft. Monmouth, N. J.
V. Contr. DA36-039-SC-89113

UNCLASSIFIED

AD Div. 8/4, 14/11, 17/9

Sperry Microwave Electronics Company, Division of Sperry Rand Corporation, Clearwater, Florida.
STUDY OF PULSED RADIATION EFFECTS ON MICROWAVE FERRITE DUPLEXERS. By J. P. Scheiwe, G. R. Harrison. Third Quarterly Report - 1 November 1962 to 31 January 1963. [illegible] pp Inc. Illus-Graphs, 14 refs. (Rept. No. SJ-222-004-3)

Contract DA36-039-SC-89113 Unclassified Report

This report presents the results from the second series of radiation environment experiments conducted during the third quarter of the program. These experiments were performed to substantiate and extend the data on the duplexer components' behavior obtained during the first series of experiments. Data are also presented from preliminary investigations of the radiation effects in waveguide elements (which might be required for future high power tests) and static dc voltage experiments which were conducted to simulate possible high microwave power electric field intensities.

Briefly described and reviewed are procedures for testing the coaxial ferrite Y-junction circulator, the gyromagnetic coupling limiter, the internal magnet coaxial isolator and C-band waveguide elements at a microwave power of 100 milliwatts in the frequency range of 5.4 to 5.9 Gc. Also reviewed is the method used to perform the static dc voltage experiments involving tests of the microwave components mentioned above, various open ended connectors (potted and unpotted) and short pieces of open ended cable.

Photographs of oscilloscope traces showing radiation effects on the operating characteristics of the microwave components and leakage characteristics of the components used in the dc experiments are presented. Quantitative interpretations of the data obtained by circuit calibration procedures are also presented.

Results of dosimetry provided by the SPRF are tabulated along with the radiation effects noted in the components investigated in each experiment.

UNCLASSIFIED

1. Pulsed Radiation Effects in Ferrite Duplexers
2. Duplexers, C-Band
3. Circulator, ferrite
4. Gyromagnetic coupling ferrite limiter
5. Isolator, ferrite

I. Radiation effects
II. Scheiwe, J. P.
III. Harrison, G. R.
IV. U. S. Army Electronics R&D Laboratory, Ft. Monmouth, N. J.
V. Contr. DA36-039-SC-89113

UNCLASSIFIED

AD Div. 8/4, 14/11, 17/9

Sperry Microwave Electronics Company, Division of Sperry Rand Corporation, Clearwater, Florida.
STUDY OF PULSED RADIATION EFFECTS ON MICROWAVE FERRITE DUPLEXERS. By J. P. Scheiwe, G. R. Harrison. Third Quarterly Report - 1 November 1962 to 31 January 1963. [illegible] pp Inc. Illus-Graphs, 14 refs. (Rept. No. SJ-222-004-3)

Contract DA36-039-SC-89113 Unclassified Report

This report presents the results from the second series of radiation environment experiments conducted during the third quarter of the program. These experiments were performed to substantiate and extend the data on the duplexer components' behavior obtained during the first series of experiments. Data are also presented from preliminary investigations of the radiation effects in waveguide elements (which might be required for future high power tests) and static dc voltage experiments which were conducted to simulate possible high microwave power electric field intensities.

Briefly described and reviewed are procedures for testing the coaxial ferrite Y-junction circulator, the gyromagnetic coupling limiter, the internal magnet coaxial isolator and C-band waveguide elements at a microwave power of 100 milliwatts in the frequency range of 5.4 to 5.9 Gc. Also reviewed is the method used to perform the static dc voltage experiments involving tests of the microwave components mentioned above, various open ended connectors (potted and unpotted) and short pieces of open ended cable.

Photographs of oscilloscope traces showing radiation effects on the operating characteristics of the microwave components and leakage characteristics of the components used in the dc experiments are presented. Quantitative interpretations of the data obtained by circuit calibration procedures are also presented.

Results of dosimetry provided by the SPRF are tabulated along with the radiation effects noted in the components investigated in each experiment.

UNCLASSIFIED

1. Pulsed Radiation Effects in Ferrite Duplexers
2. Duplexers, C-Band
3. Circulator, ferrite
4. Gyromagnetic coupling ferrite limiter
5. Isolator, ferrite

I. Radiation effects
II. Scheiwe, J. P.
III. Harrison, G. R.
IV. U. S. Army Electronics R&D Laboratory, Ft. Monmouth, N. J.
V. Contr. DA36-039-SC-89113

UNCLASSIFIED

AD Div. 8/4, 14/11, 17/9

Sperry Microwave Electronics Company, Division of Sperry Rand Corporation, Clearwater, Florida.
STUDY OF PULSED RADIATION EFFECTS ON MICROWAVE FERRITE DUPLEXERS. By J. P. Scheiwe, G. R. Harrison. Third Quarterly Report - 1 November 1962 to 31 January 1963. [illegible] pp Inc. Illus-Graphs, 14 refs. (Rept. No. SJ-222-004-3)

Contract DA36-039-SC-89113 Unclassified Report

This report presents the results from the second series of radiation environment experiments conducted during the third quarter of the program. These experiments were performed to substantiate and extend the data on the duplexer components' behavior obtained during the first series of experiments. Data are also presented from preliminary investigations of the radiation effects in waveguide elements (which might be required for future high power tests) and static dc voltage experiments which were conducted to simulate possible high microwave power electric field intensities.

Briefly described and reviewed are procedures for testing the coaxial ferrite Y-junction circulator, the gyromagnetic coupling limiter, the internal magnet coaxial isolator and C-band waveguide elements at a microwave power of 100 milliwatts in the frequency range of 5.4 to 5.9 Gc. Also reviewed is the method used to perform the static dc voltage experiments involving tests of the microwave components mentioned above, various open ended connectors (potted and unpotted) and short pieces of open ended cable.

Photographs of oscilloscope traces showing radiation effects on the operating characteristics of the microwave components and leakage characteristics of the components used in the dc experiments are presented. Quantitative interpretations of the data obtained by circuit calibration procedures are also presented.

Results of dosimetry provided by the SPRF are tabulated along with the radiation effects noted in the components investigated in each experiment.

UNCLASSIFIED

1. Pulsed Radiation Effects in Ferrite Duplexers
2. Duplexers, C-Band
3. Circulator, ferrite
4. Gyromagnetic coupling ferrite limiter
5. Isolator, ferrite

I. Radiation effects
II. Scheiwe, J. P.
III. Harrison, G. R.
IV. U. S. Army Electronics R&D Laboratory, Ft. Monmouth, N. J.
V. Contr. DA36-039-SC-89113

UNCLASSIFIED